IRE Transactions on AUDIO

VOLUME AU-3 SEPTEMBER-OCTOBER, 1955 NUMBER 5

Published Bi-Monthly

CONTENTS

PUBLISHED BY THE

Professional Group on Audio

PGA News

NEC AUDIO SESSIONS

The PGA is sponsoring an Audio Session at the National Electronics Conference, which is being held this year at the Hotel Sherman in Chicago, on October 3, 4, and 5. The specific date and location of the Audio Session was not available at the time this issue went to press, but the program had been tentatively set as follows:

The Electrostatic Loudspeaker
Robert J. Larson, *speaker*
Jensen Manufacturing Co.

Efficiency and Power Rating of Loudspeakers
R. W. Benson, *speaker*
Armour Research Foundation

Bells, Electronic Carillons, and Chimes
F. H. Slaymaker, *speaker*
Stromberg-Carlson Co.

Energy Content of Recorded Music
John Overly, *speaker*
Electro-Voice

Reference to the NEC Program, which is available now, will yield more specific information.

IRE-PGA CHAPTER ACTIVITIES

Albuquerque, N. M.

During the 1954-1955 season the Albuquerque Section of the PGA held ten meetings with an average attendance of 38 per meeting. At the last meeting of the season, on June 13, 1955, Mr. Bob McDonald of Sound Engineer presented a discussion and demonstration on "Three Basic Speaker Enclosures." At this same meeting the following officers were elected for the coming year: Hoyt Westcott, *Chairman*, and Ben Lawrence, *Secretary-Treasurer*.

The Albuquerque Chapter recently issued a publication entitled "Equalization Characteristics of Various Disc Recordings." Copies of this publication, together with the following past publications are in the Chapter files: "Audio Amplifier Trouble Shooting," "Crossover Network Design," "Blonde Finish for Oak," "Baruch-Lang Construction Details," "R-J Construction Details."

Syracuse, N. Y.

On April 13, 1955, Mr. A. F. Petrie of the General Electric Co. presented a paper on "Performance of the 'Distributed Port' Loudspeaker Enclosure." The paper concluded with a demonstration showing the effect of enclosures and ports on low-frequency performance.

On May 17, 1955, Mr. Sig. Zuerker, also of the General Electric Co., spoke on "The new G.E. Type A1-400 High-Fidelity Loudspeaker." Mr. Zuerker developed electro-mechanical circuit analogies for the low and high ends of the woofer and tweeter, respectively. The talk concluded with a demonstration of music reproduction from high-fidelity records.

Officers elected for the coming year are D. E. Maxwell *Chairman*, and W. W. Dean, *Secretary*.

Boston, Mass.

The final paper scheduled for this season, "Man, a Somewhat Neglected Component of Hi-Fi Systems," dealt with a subject of considerably more basic import than the casual nature of its title might suggest, since it is the listener who passes final judgment on the success or failure of all audio developments; the speaker was Professor Walter A. Rosenblith of MIT, a nationally recognized authority on the electrophysiology of hearing, and on the psychoacoustic interactions between sound and man.

Attendance at the meetings this season has averaged approximately fifty-five persons. An unusually high degree of interest expressed by our guests in IRE and PGA membership suggests a continuing enthusiasm for Audio Chapter activities and a growing participation and membership during the years ahead.

Cincinnati, Ohio

At the yearly dinner and meeting of the Cincinnati Section in June, the following members were elected to serve as PGA officers for the coming year: J. Park Goode, *Chairman;* Richard H. Lehman, *Vice-Chairman;* E. Dilworth Kay, *Secretary-Treasurer*.

Chapter News

News of a PGA Chapter activities should be sent to A. Preisman, Capitol Radio Engineering Institute, Washington, D.C., by the first of each odd month of the year. The chapters themselves must furnish the chapter news if they want it to appear in print.

WITH THE ACOUSTICAL SOCIETY

THE May, 1955, issue of the *Journal of the Acoustical Society of America* (Vol. 27, No. 3) contains 32 papers on acoustical subjects. Eight of them will be of special interest to many members of the IRE-PGA. They are as follows:

"Measurement of Difference in Loudness Between Typing Noises," by Joseph Abruzzo, p. 457. It is difficult to ascertain the absolute loudness of typing noise by objective measurement. Difference in loudness between typing noises can often be measured with practical accuracy by means of a sound-level meter.

"Semiplastic Earplugs," by J. Zwislocki, p. 460. Description of the development of an earplug with soft

elastic walls and a viscous core malleable at body temperature. One size fitted 90 per cent of the ears of the 25 people tested sufficiently well.

"Measurements of Hearing Acuity Among Submariners and Noise Levels in Working Compartments," by J. C. Webster and L. N. Solomon, p. 466. To study the prevalence of hearing losses among submariners, and their possible causes and consequences, the NEL warble tone hearing test was administered to 1,053 submariners.

"Isomorphisms between Oriented Linear Graphs and Lumped Physical Systems," by Horace M. Trent, p. 500. A unifying principle is presented whereby all finite lumped systems can be analyzed by a single technique, no matter how complex the system may be. Formal procedures for establishing complete analogies are presented.

"Thickness Measurement by Ultrasonic Resonance," by E. G. Cook and H. E. Van Valkenburg, p. 564. A mathematical analysis is made of the acoustic system of resonance-type instruments used for thickness measurements from one side only.

"Survey of Flux-Responsive Magnetic Reproducing Heads," by Otto Kornei, p. 575. Paper reprinted from July, 1954, *Journal of the Audio Engineering Society*. A review of magnetic reproducing heads which generate a signal voltage substantially proportional to the magnitude of the intercepted magnetic flux.

"Calibration of Test Records by Interference Patterns," by B. B. Bauer, p. 586. Mathematical derivations of interference patterns of test records, useful for determination of record amplitude and frequency.

"Electronic Music Synthesizer," by Harry F. Olson and Herbert Belar, p. 595. The electronic music synthesizer is a machine that produces music from a coded record. The musician, musical engineer, and composer are provided with a new musical tool with no inherent physical limitations.

In addition, the issue contains its usual extensive "References to Contemporary Papers on Acoustics," by Robert T. Beyer and "Review of Acoustical Patents," by Robert W. Young.—B. B. Bauer, Associate Editor, Jour. of the Acous. Soc. of Amer.

An Improved Optical Method for Calibrating Test Records*

B. B. BAUER†

Test records are often calibrated by measuring the width of the optical pattern formed when a sharp beam of light is reflected from the Modulated grooves. An error has been found in this measurement owing to diffraction of light at the edges of the pattern, which results in a fuzzy ending and a general enlargement of the pattern width, especially at high frequency. A new optical method has been devised for calibration of test records by the use of interference-line patterns. Two sets of interference lines have been identified: (a) Uniformly spaced lines which are related to the recorded frequency, the angular velocity of the record, and the wavelength of light (these have been called the *A* lines); (b) lines with variable spacing which are related to the amplitude of modulation and to the wavelength of light (these have been called the *B* lines). *B*-line patterns may be readily related to the theoretical width of the optical pattern free of diffraction error, with the resultant improvement in the accuracy of test-record calibration.

Introduction

THE CALIBRATION of test records is a central problem in the art of phonograph reproduction. In 1930 Buchmann and Meyer proposed an optical method of performing this calibration.[1] Their method was based upon the observation that the optical pattern obtained when a sharp beam of light is reflected from the record is widest at the portions of maximum modulation. Buchmann and Meyer reasoned that the furthermost reflection at either side of the optical pattern occurs at the points where the maximum slope of groove modulation is perpendicularly oriented with respect to the source of light and the eye of the observer. At that particular point, the angle subtended by the pattern with respect to the line of symmetry through the center of the record is the same as the slope of the groove modulation, and a bit of analysis shows that the following approximate relation exists (Fig. 1):

$$v = \pi n b. \tag{1}$$

Here v is the velocity in cm per second maximum, if b is the width of pattern in cms, and n is the rps of the disc.

Since the radius of the groove r or modulation frequency f are not contained in this equation, one might deduce from it that the pattern will remain constant in width for constant velocity of groove modulation, without regard for the frequency of the recorded sound or groove radius. In 1946 the writer demonstrated[2] that the above relationship is fulfilled only when the source of light and the observer are located at virtual infinity from the record. In the more usual case of a proximate observer and/or source of light, the pattern farthest away from the source widens to a new width b_0, and that nearest to the source narrows down to a width b_i. These patterns are called the "outer" and the "inner" pattern, respectively, as they are caused by reflections from the outer and the inner walls of the groove. For the case of the proximate observer, the following approximate equation is applicable:

$$v = 2\pi n b_0 b_i/(b_0 + b_i). \tag{2}$$

It should be noted that this equation does not contain a frequency term, and it, likewise, is independent of the radius of the groove as long as b_0 and b_i are measured on the same radius.

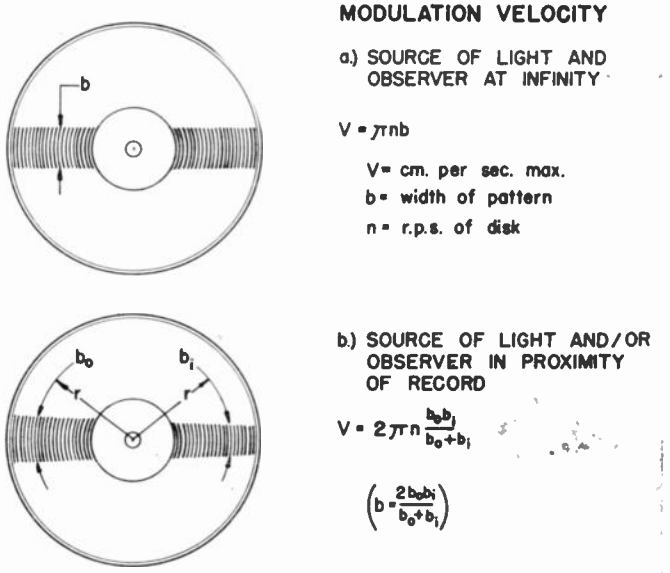

Fig. 1—Measurement of modulation velocity by light patterns.

Up to this point one might conclude that calibration of test records by either of the above equations is a very simple matter. Actually, the real problem is that of measuring the pattern width. The ends of the pattern are not sharply defined: Instead, the illumination drops off gradually and it is hard to determine where the pattern ends. For relative measurements, some assistance is obtained by photographing the pattern, because the short contrast scale of the film helps to produce a sharp cutoff. Without further analysis, one is not sure, however, to what degree this cutoff affects the absolute calibration of the record. Even this expedient is not always satisfactory, because different grooves are apt to reflect the light in varying manner. This paper is concerned, to a large degree, with the development of a more accurate method for measuring the true width of light patterns for use in the preceding equations.

* Presented, IRE National Convention, March 21, 1955.

† Vice-President and Director of Research, Shure Brothers, Inc., Chicago 10, Ill.

[1] G. Buchmann and E. Meyer, "A new optical method of measurement for phonograph records," E.N.T. 7, 147 (1930), Translated, *Jour. Acous. Soc. Am.*, vol. 12, p. 303, 1940.

[2] B. B. Bauer, "Measurement of recording characteristics by means of light patterns," *Jour. Acous, Soc. Am.*, vol. 18, pp. 387–395; October, 1946.

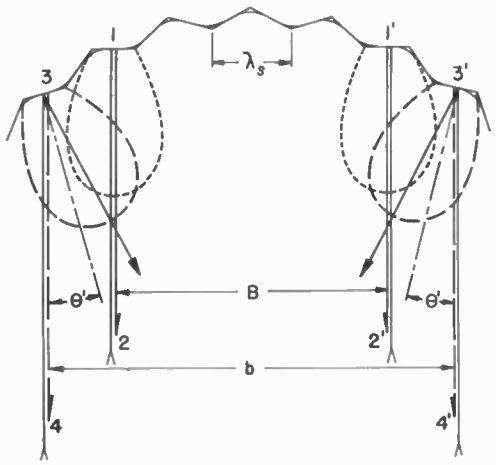

Fig. 2—Diffraction error at edges of pattern.

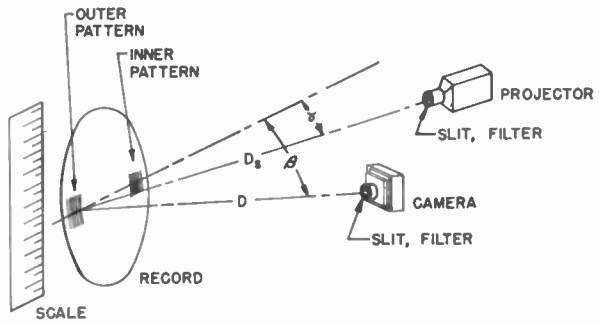

Fig. 3—Technique for photographing interference light patterns.

Diffraction Patterns

Visual observations of light patterns through color filters revealed that they are narrowed down by the use of blue light, as compared to white or red light, and this was the first indication of the existence of a substantial diffraction error.

Let us examine the nature of this diffraction error. In Fig. 2 is shown a single modulated groove with the source of light and the observer placed at infinity—downward. Reflection points 1 and 1′ are the farthest portions of the groove wall in confronting relationship with the line of sight of the observer, as indicated by the arrows 1–2 and 1′–2′. By the Buchmann-Meyer theory, the distance between 1 and 1′ enables us to calculate the slope of the modulated wave and, hence, the velocity of modulation. However, when reflection takes place from these small surfaces, the light is diffracted with the principal order of diffraction spreading out in the form of the dotted lobes shown emanating from 1 and 1′. Owing to this diffraction, the points beyond 1 and 1′ also become visible, until we reach some points 3 and 3′ where the principal diffraction lobes (shown in dash lines) present a null in the direction of the line of sight of the observer. By assuming triangularly modulated grooves, it is simple to approximate the order of magnitude of this diffraction and obtain a result in rough agreement with experiment.[3]

The measurement of the manifest width of pattern b, as practiced with conventional light patterns, takes place between the points 3 and 3′, resulting in a measure-

[3] B. B. Bauer, "Calibration of test records by interference patterns," *Jour. Acous. Soc. Am.*, pp. 586–594; May, 1955.

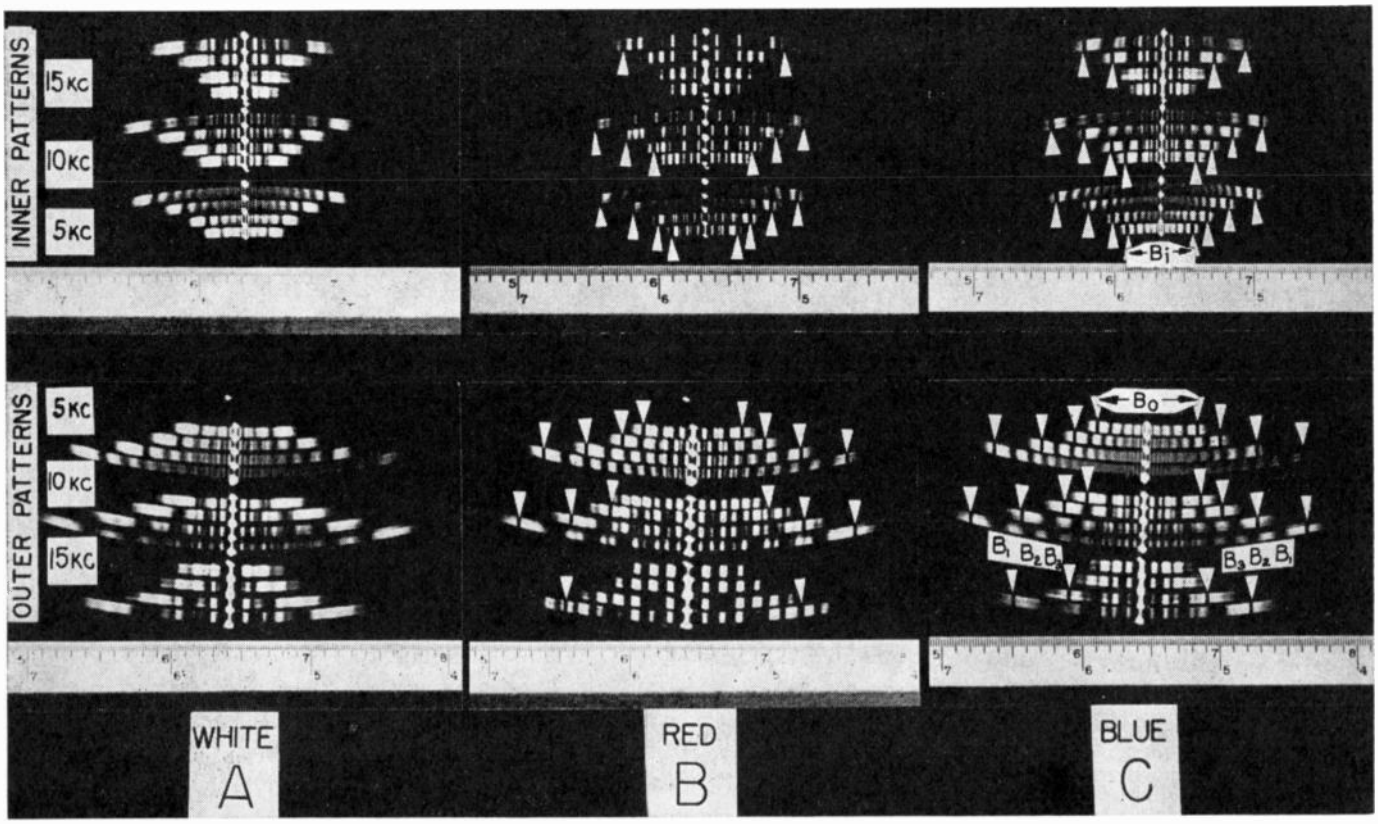

Fig 4—Interference light patterns for special record containing 5-, 10- and 15-kc bands.

ment which is too large. Thus, we are confronted with the question, "How to obtain the theoretical pattern width, B?"

To study the effects of dispersion and diffraction, our photographic technique was refined as shown in Fig. 3. By placing a slit 3/16-inch wide over the projector lens, and a 0.1-inch slit over the camera lens, and with suitable slit orientation, the pattern sharpens remarkably.[4] By the use of color filters over the projector or camera lens, individual interference lines become clearly visible.

As an example of the results obtained by this technique, Fig. 4 is a photograph of the patterns reflected from a record cut at our request by William Putnam, of the Univeral Recording Studio, Chicago, Ill., whose cooperation in this connection is gratefully acknowledged. This record has three sets of frequency bands of 15, 10, and 5 kc each, respectively. The bands in each set differ from each other by approximately 3 db. From left to right are the photographs by white light, with red, and with blue filters, respectively. A scale divided into 50ths-of-an-inch has been placed along side the record for measurement purposes.

We observe the existence of two distinct patterns of lines. Close to the center of each band there are equidistant lines which do not appear to be affected by the amplitude of modulation or by the radius of the groove, but which are affected by the recorded frequency and by the color of light; I have called them the A lines. There is a second pattern of lines, best seen close to the edges of the bands, which are unevenly spaced and which are influenced by the amplitude of modulation. I have called them the B lines. For example, the first three B lines of the longest blue 10-kc band are labeled underneath as B_1, B_2, B_3.

The B lines have been observed to exhibit the following interesting property hereinafter explained: if the distance between the lines B_1 and B_2 is scaled off from B_1 towards the edge of the pattern, the location of the theoretical end of the pattern is found. This operation was performed for all the red and blue patterns and the location of the theoretical ends of the pattern is shown by the triangular white markers. That portion of the pattern beyond the confines of the markers is caused by diffraction of light at the edges of the pattern, as explained before.

The distance between the corresponding markers is called the "B-line pattern width" and it is the width to be used with the preceding equations for obtaining the velocity of groove modulation, free of diffraction error. The B-line pattern width for the outer patterns has been called B_0 to distinguish it from the B-line width of the inner pattern called B_i. B_0 and B_i have been indicated, by the way of example, for the smallest 5-kc blue-band.

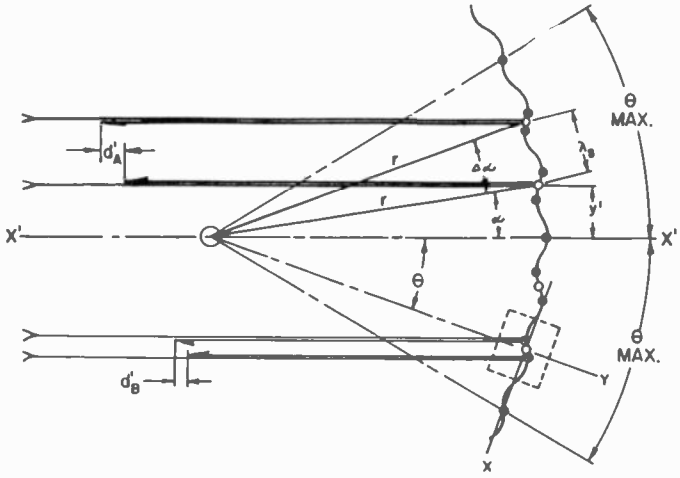

Fig. 5—Geometry of modulated groove for explanaing A- and B-line patterns.

Analysis of the A and B lines

The nature of A and B lines is revealed by examining the geometry of a modulated groove, shown in Fig. 5. For simplicity, it is assumed that the groove wall is vertical, and the source of light and the observer are at left, at virtual infinity. The light pattern is formed by reflections which take place each time the groove modulation is perpendicular to the $X'-X'$ axis. These points of reflection are shown by black dots. Assume, for the time being, that each pair of adjacent points of reflection acts as a single intermediate reflection shown by a white dot. These white dots are one modulation wavelength λ_s apart. To calculate the resulting interference pattern, one must find the positions along the groove wall where the difference of path of reflection, d_A', between two successive white dots is equal to an odd multiple of half the wavelength of light. One of the steps in the derivation is the provision of a correction factor to account for the inclination of the groove in the case of a real record. For the infinite observer and light source the approximate equation defining the spacing of A lines A is as follows:[3]

$$A = \lambda_L f/2\pi n(\cos\gamma + \cos\beta) \qquad (3)$$

where

A is the spacing of the A lines, cm.
f is the frequency of the recorded sound, cps.
λ_L is the wavelength of light, cm.
n is the rotational speed, rps.
γ and β are the angles of incidence and reflection with respect to the surface of the disc.

[4] A similar effect may be obtained by use of smaller F stop, but with considerable loss of light. Recently it has been called to the author's attention that the nature of the dispersion and diffraction effects have been described by Axon and Geddes ("The calibration of disc recordings by light pattern measurements," *Proc. I.E.E.*, vol. 100, Part III; July 1953). They do not associate the distribution of interference lines with a theoretical pattern width B. Instead they compute the intensity distribution of the image of the pattern formed at the focal plane of the groove. This intensity, they found, falls to half of the maximum value at the theoretical ending of the pattern. They thereupon describe an ingenious instrument based upon the principle of the sextant which provides a measurement of the image widths based on the observation that the two superimposed images visible in the sextant blend into one continuous image of uniform intensity.

We find the spacing between the A lines is proportional to the frequency and the wavelength of light, and inversely proportional to the rps of the record. A lines may be used, therefore, to estimate one of the wavelength of light, frequency of modulation, or the angular speed of the record, if the other two are known.

In the case of the proximate observer or light source, the outer A-line spacing widens and becomes A_0, and the inner A-line spacing narrows down and becomes A_i. A is found from the equation:

$$A = 2A_0A_i/(A_0 + A_i). \quad (4)$$

Thus, with the aid of A lines, a test record may be used as a diffraction grating, but this property is not especially helpful in calibrating test records!

The lower portion of Fig. 5 is pertinent to the derivation of B lines. We have considered above that the adjacent points of reflection act as a single reflection. However, when the difference of paths d_B' between any such two points becomes equal to an odd multiple of half the wavelength of light there will be a cancellation of intensity. Thus the B-line pattern may be considered as an amplitude modulation of the A-line pattern.

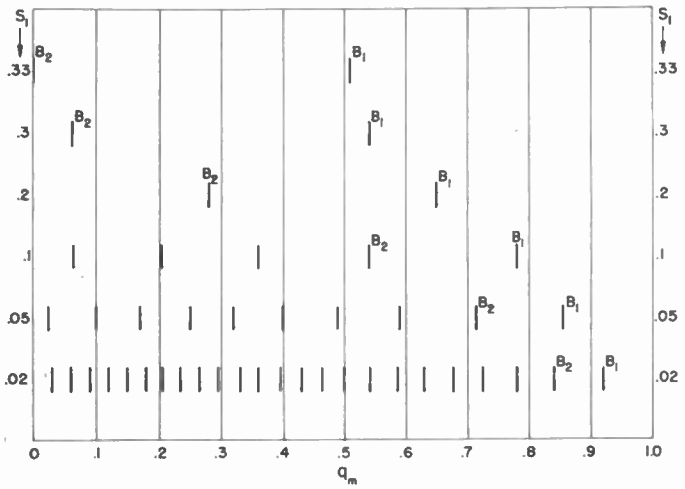

Fig. 6—Typical B-line pattern for various values of S_1.

To derive the equation for B lines it is necessary to express d_B' as a function of the angle θ, which is the angular location of a given wavelet, and the angle θ_{max} which is the angular location of the theoretical end of the pattern from the line of symmetry; and further, to include the correction for the inclination of the groove. With the use of some approximations to make the equation more manageable without the introduction of undue error, the following relation is obtained:[3]

$$S_m = (1 - q_m^2)^{1/2} - q_m \sin^{-1}(1 - q_m^2)^{1/2} \quad (5)$$

where

$S_m = \lambda_L(-\frac{1}{2} + m)/2a(\cos\gamma + \cos\beta)$
$m = 1, 2, 3, \cdots$
$q_m = \theta_m/\theta_{max}$
a = amplitude of modulation
θ_m = angular location of the m'th line
γ and β are the angles of incidence and reflection of light relative to the record surface.

With the help of the above equation a series of B-line patterns was calculated, using representative values of S_1, (i.e., the S_m corresponding to $m = 1$). This series appears in Fig. 6. On a relative scale, the abcissa represents the angular position of lines B_1, B_2, etc., with respect to θ_{max} taken as unity, for the various values of S_1 listed along the sides of the figure. We observe that the space between the lines B_1 and B_2 is very nearly equal, in all these patterns, to the space between the theoretical end of the pattern and B_1. This observation is the basis for the assertion made earlier and which can now be summarized by the following rule:

Rule 1: The theoretical width of a light pattern is obtained by adding to the outer B lines a measure equal to the distance between the first and the second B lines.

Calibration of Test Records

As an example of B-line pattern calibrations, Fig. 7 shows the interference pattern for Cook 10 LP $33\frac{1}{3}$-rpm record with frequency bands up to 20 kc, taken with

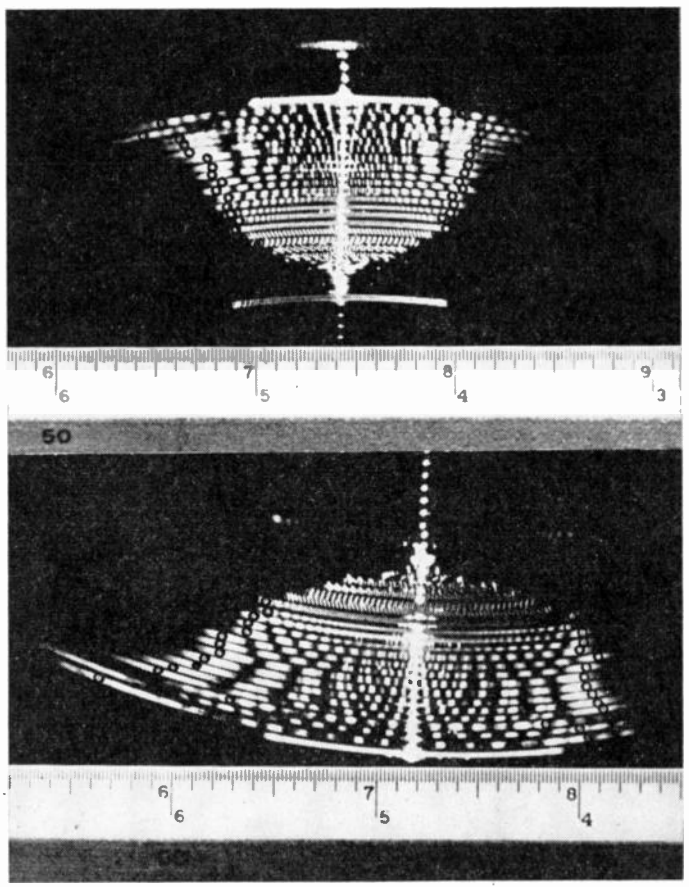

Fig. 7—Interference patterns for Cook 10 LP test record ($33\frac{1}{3}$ rpm).

red filter. The *B*-line pattern widths were determined for each frequency band, by Rule 1, and the theoretical terminals of each band are shown by small circles. For comparative purposes, the over-all pattern widths were also measured. The resulting calibrations are shown in Fig. 8. The crosses represent the conventional light pattern calibration. The small circles portray the *B*-line pattern calibration. As an approximate check, this record also was calibrated by the variable turntable technique and the Kornei correction for the playback loss owing to the yielding of the groove was calculated.[5]

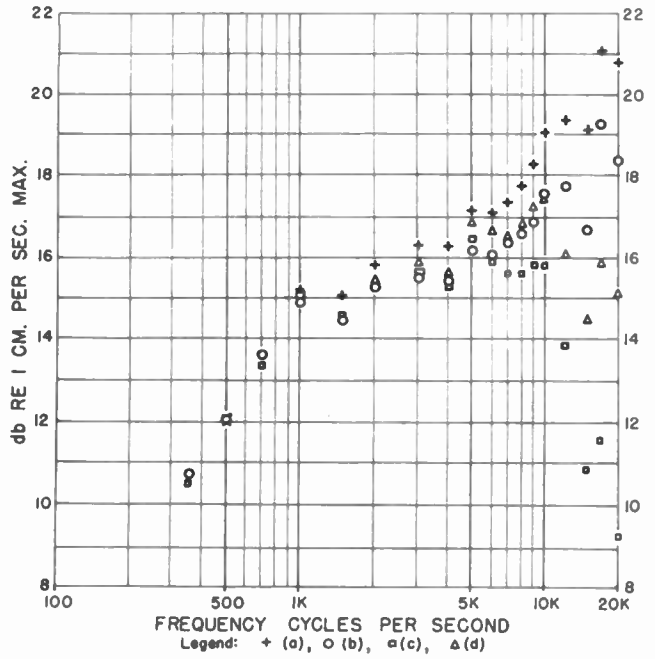

Fig. 8—Calibration for Cook No. 10 LP (33⅓ rpm) record by: (a) conventional light pattern method; *B*-line pattern method; (c) variable speed turntable method; (d) Kornei correction computed for the latter.

The squares represent the calibration by the variable turntable technique, and the triangles denote the addition of the Kornei correction. The *B*-line pattern calibration, and the variable turntable method with the Kornei correction are within ½ db of each other up to 10 kc, and with 3 db up to 20 kc.

Fig. 9 shows the interference pattern for the Cook 10—78-rpm record with upper frequency limit of 20 kc. Fig. 10 portrays the response-frequency characteristics calculated from this pattern. The crosses again denote conventional light-pattern calibration; the circles, the *B*-line pattern calibration, and the triangles the variable turntable calibration with the Kornei correction added. It is seen that, in this instance, there is agree-

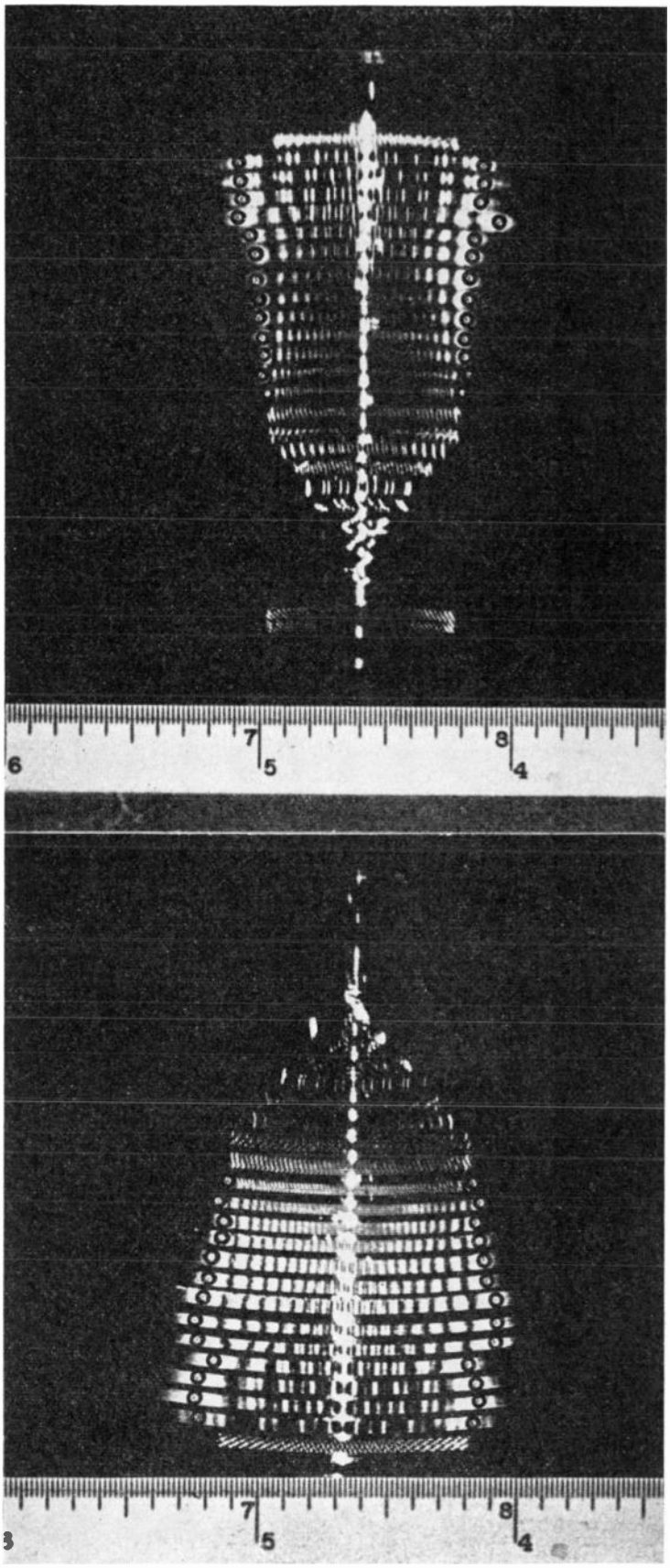

Fig. 9—Interference patterns for Cook No. 10 (78 rpm) test record.

[5] O. Kornei, "On the playback loss in the reproduction of phonograph records," *Jour. Soc. Motion Picture Eng.*, vol. 37, pp. 569–590; 1941.

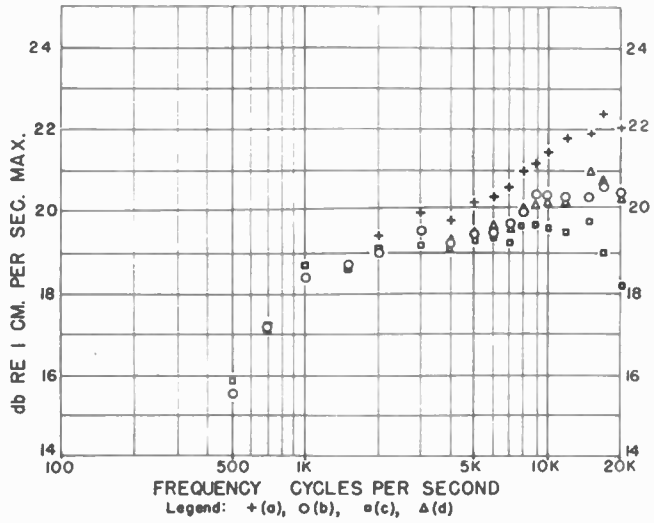

Fig. 10—Calibration of Cook No. 10 (78 rpm) record by: (a) conventional light pattern method; (b) *B*-line pattern method; (c) variable speed turntable method; (d) Kornei correction computed for the latter.

ment between the last two calibrations within about ½ db up to 20 kc. A number of other similar measurements showed that *B*-line patterns provide trustworthy calibrations.

Fig. 11 shows the interference-line pattern for the RCA 45-rpm record No. 12-5-31. Small circles again have been drawn to indicate the theoretical ending of the pattern. Fig. 12 shows the conventional and the *B*-line pattern calibration of the record. Thus, it is seen that a record which might have been previously thought to have a constant velocity characteristic to 10 kc, actually has a slightly falling characteristic at high frequency.

It should be noted that the difference in calibration obtained by conventional light-pattern method, and by the *B*-line pattern method is of the order of 1½ db at 10 kc and about 3 db at 20 kc. Further analysis has disclosed that the error in the conventional light-pattern measurements is apt to be approximately 0.15 cm per second per kc. It is evident that the conventional light pattern should widen slightly toward the high frequency to provide a constant velocity characteristic.

One useful observation is directed to the fact that the theoretical ending of the pattern is located at or near the brightest portion of the last bright band at either end of the pattern. This suggests the possibility of the future development of some photographic or photometric method for determining automatically the correct pattern width.

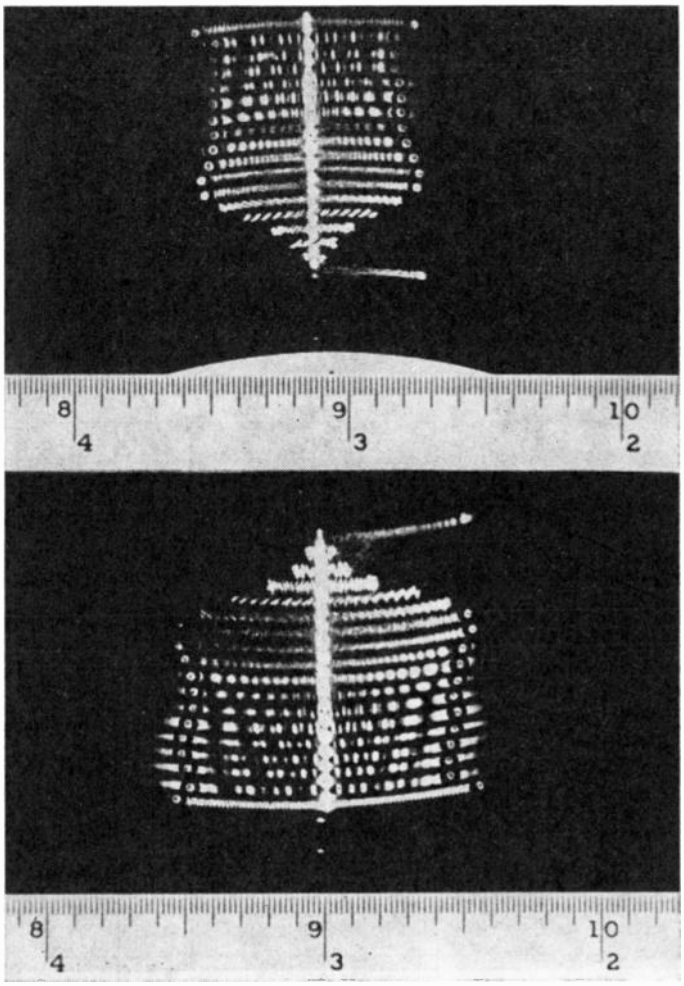

Fig. 11—Interference patterns for RCA record 12-5-31.

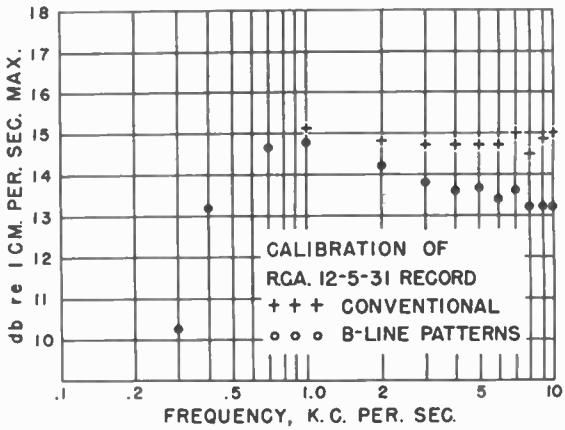

Fig. 12—Calibration of RCA record 12-5-31 by conventional light patterns and by *B*-line patterns.

Conclusion

In conclusion, it is now possible to ascertain the complete velocity-frequency characteristic of an unknown test record by purely optical means. This comes about from the study of interference patterns, which has given us (1) a better understanding of the nature of light-patterns; (2) the means for measuring the recorded frequency in terms of the wavelength of light, or vice versa; and (3) an improved technique for calibrating records by removing the uncertainty in the measurement of pattern width, and by eliminating errors caused by diffraction.

Design Principles of Junction Transistor Audio Amplifiers*

R. L. TRENT†

The junction transistor may be represented as an active network in terms of various two-terminal pair equivalent circuits. The principles of design of audio-frequency amplifiers consisting of one or more transistor stages may be outlined in terms of these equivalent circuits. The effects of applying feedback to the amplifier configurations are discussed. Various methods for minimizing drifts of the quiescent point of operation of transistor amplifier stages are considered. Signal-to-noise ratios, important in the design of high quality amplifiers, are developed in terms of device noise figures.

Introduction

THE PRECEDING paper[1] of this series on the audio-frequency aspects of junction transistors discussed fundamental electronic mechanisms underlying transistor action, and introduced various two-terminal pair equivalent circuits capable of representing the transistor as an active network. Analytical expressions for small-signal audio-frequency operation in each of the three basic methods of connection of the device in a circuit were developed.

With this background, it is proposed in this paper to discuss the principles underlying the design of amplifiers made up of one or more transistor stages. The basic feedback relationships will be developed, and the effects of applying feedback to the amplifier configurations will be discussed. It will be shown that feedback has the same virtues when applied to transistor amplifiers as to electron tube amplifiers. Consideration will be given to various methods for minimizing drifts of the quiescent point of operation of transistor amplifier stages.

The noise problem, which is important in the design of high-quality amplifiers, will be treated in terms of device noise figures and amplifiers signal-to-noise ratios.

Classification of Amplifiers

Transistor audio amplification stages may be classified in a manner analogous to that used for electron tube amplifiers. The operation may be class A, AB, B, or C, etc., depending upon the conduction angle of the output signal current. Biasing conditions and input current amplitudes typical of the various classifications are illustrated in Fig. 1 for a common base connected stage.

Thus class-A operation implies emitter dc biasing to achieve a quiescent operating point on the linear portion of the dynamic current transfer characteristic, with input current excursions proportioned so that the linear portion of the characteristic is not exceeded. Output signal current flows during the entire input cycle. For class-B operation, the emitter dc current biasing condition is set approximately at collector current cutoff.

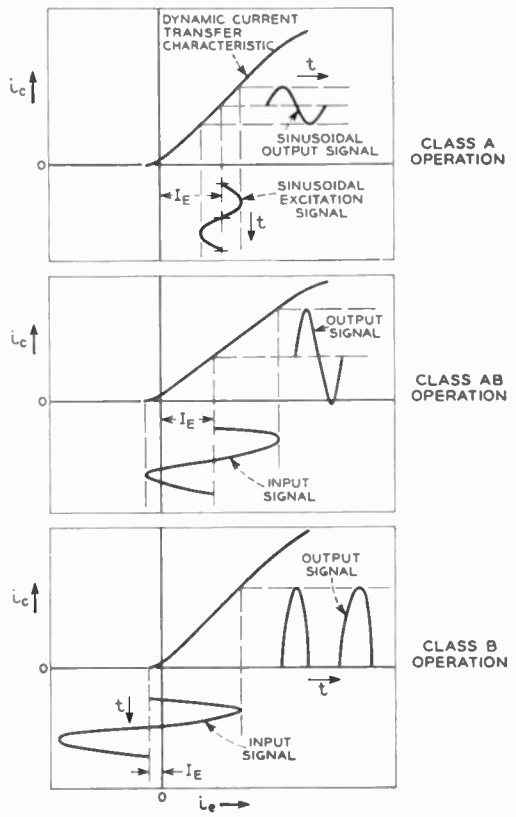

Fig. 1—Amplifier classifications.

In this case output signal current flows only during the positive one-half cycles of the excitation current waveform.

Due to the low output distortion requirements ordinarily imposed on audio-frequency amplifier stages, they are usually operated class A, except for power output stages. In the latter case,[2] push-pull operation and the use of appropriate amounts of degenerative feedback makes class -B or -AB operation possible without exceeding usual minimum distortion requirements. This type of operation permits more efficient power conversion in a fashion analogous to that of the corresponding electron tube connections.

Static Characteristic Families

Familiarity with the various static characteristic families usually illustrated for the junction transistor is of fundamental importance in circuit design. These

* Manuscript received June 18, 1955. *Note:* This is the second of a group of three tutuorial papers on transistors, with special emphasis on use at audio frequencies, prepared by the Bell Telephone Laboratories Staff at the request of the editorial committee of the Transactions on Audio. The first paper, "Properties of Junction Transistors," by R. J. Kircher, appeared in the July-August issue. The third "Design Principles for Junction paper, Transistor Audio Power Amplifiers," by D. R. Fewer, will appear in a succeeding issue of this publication.

† Bell Telephone Laboratories, Murray Hill, N. J.

[1] R. J. Kircher, "Properties of junction transistors," TRANS. IRE, Vol. AU-3, pp. 107–124; July–August, 1955.

[2] D. R. Fewer, "Design principles of junction transistor audio power amplifiers,"—To be published in TRANS. IRE—Audio.

curves are useful in determining practical limits of operation in terms of maximum allowable power dissipations and ambient temperatures, distortion effects, and small signal amplification factors.

The most commonly used set of transistor static characteristics is the collector or output family. Representative output characteristics for the common base connection are shown in Fig. (2a). Collector voltage with respect to the base (V_{CB}) is plotted against collector current for fixed values of constant emitter current. The slopes[1] of these curves correspond to the small signal parameter $r_{22}=r_c+r_b$.

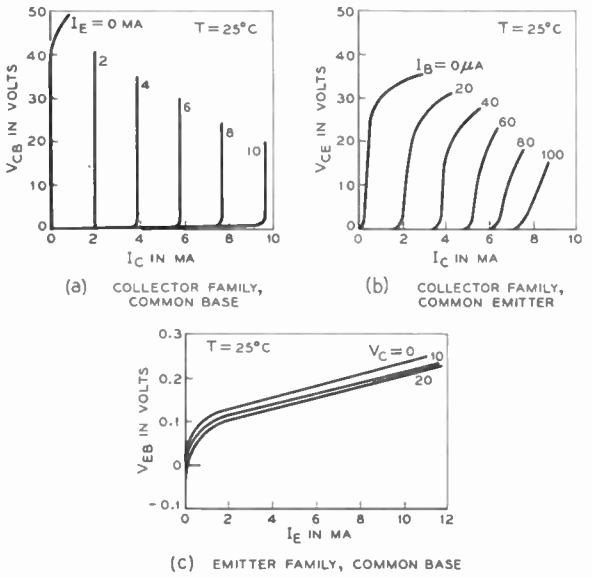

Fig. 2—Static characteristics families; (a) collector family common base; (b) collector family common emitter; and (c) emitter family common base.

In Fig. 2(b), typical output characteristics for the common emitter connection are shown, in which collector voltage (V_{CE}) is plotted against collector current for fixed values of constant base current. The slopes of these curves correspond to the small signal parameter $r_{22}=r_c(1-\alpha)+r_e$. The output characteristics for the common collector connection are similar to those for the common emitter, and are less often used.

Another frequently illustrated set of characteristics is the emitter or input family, as shown in Fig. 2(c), in which emitter voltage is plotted against emitter current for a fixed values of constant collector voltage. In the common base connection, the slopes of these curves correspond to the small signal parameter $r_{11}=r_e+r_b$.

These families of static characteristics may be used to arrive at several interesting observations. As mentioned previously, the slopes of the curves correspond to the small signal output and input resistances, respectively. In general, slopes and spacings of the output family for common base connection are much more uniform than those for the common emitter family.

Considering the emitter or input family, the effect of collector voltage is generally small. At low emitter currents, the relation between emitter voltage and emitter current is decidedly nonlinear. This nonlinearity is of particular importance in power amplifier stage design[2] where large excursions are encountered, since it affects the source impedance required to minimize distortion in the output waveforms.

As discussed in the previous paper,[1] most of the transistor parameters are sensitive to temperature changes. In both sets of output family plots shown in Fig. 2, the collector current-voltage curve for zero input current will move rapidly to the right, following an exponential dependency on temperature. Similarly, the slopes of the curves will be modified due to changes in the value of r_c with temperature, and the spacing between curves will vary as the current multiplication factor changes. Thus ambient temperature plays an extremely important part in the operation of transistor amplifier stages, far more so than in the case of electron tubes.

A definite limitation exists on the maximum allowable temperature at the junctions. It is common practice to give a maximum allowable junction temperature and a power dissipation rating factor expressed in terms of watts per degree Centigrade rise. A hyperbola of maximum internal power dissipation at a fixed ambient temperature may then be superimposed on the characteristic families, as shown in Fig. 3, and the derating factor used when operation at any other ambient temperature is desired. Operation above the hyperbola will result in excessive junction temperatures and eventual failure or deterioration of the device characteristics.

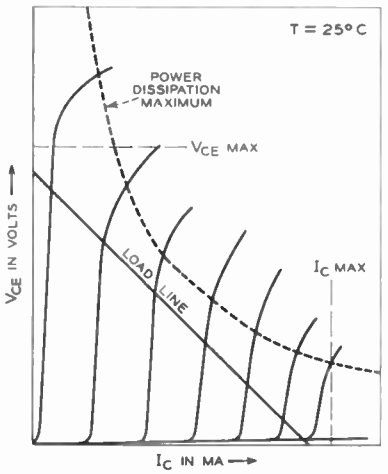

Fig. 3—Static characteristics—limits of operation.

Other limitations on the maximum excursions of collector voltage and current exist in addition to the effects of excessive internal dissipation and ambient temperature. A maximum "reverse breakdown" voltage from collector to base is usually specified, beyond which the characteristics will bend sharply denoting greatly decreased output resistance. Operating excursions[2] into such a region may result in unpredictable behavior, although compensating distortion effects may be realized. For the same type of transistor, the maximum allowable collector potential is usually less in the common

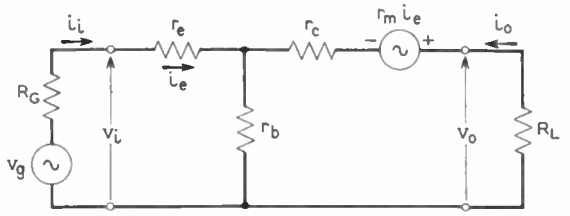

	EXACT	APPROXIMATE
INPUT RESISTANCE R_i	$r_e + r_b \frac{r_c - r_m + R_L}{r_b + r_c + R_L}$	$r_e + r_b(1-a)$
OUTPUT RESISTANCE R_o	$r_c - r_b \frac{r_m - R_G - r_e}{r_e + r_b + R_G}$	$r_c \frac{r_e + r_b(1-a) + R_G}{r_e + r_b + R_G}$
CURRENT AMPLIFICATION A_i	$\frac{i_o}{i_i} = -\frac{r_m + r_b}{r_b + r_c + R_L}$	$-a$
POWER GAIN OG	$\frac{(r_m + r_b)^2 R_L}{\left\{(r_b + r_c + R_L)\left[r_b(r_c - r_m + r_e + R_L) + r_e(r_c + R_L)\right]\right\}}$	$\frac{a^2 R_L}{r_e + r_b(1-a)}$

CONDITIONS FOR APPROXIMATE FORMULAS:

$$r_b \ll r_c,\ r_e \ll R_L \ll (r_c - r_m),\ a = \frac{r_m}{r_c} \cong \alpha$$

NOTE: SYMBOLS

(>) = CURRENT GENERATOR (∿) = VOLTAGE GENERATOR

Fig. 4—Common base stage formulas.

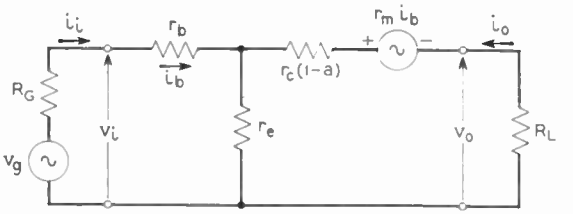

	EXACT	APPROXIMATE
INPUT RESISTANCE R_i	$r_b + r_e \frac{r_c + R_L}{r_c - r_m + r_e + R_L}$	$r_b + \frac{r_e}{1-a}$
OUTPUT RESISTANCE R_o	$r_c - r_m + r_e \frac{r_b + r_m + R_G}{r_b + r_e + R_G}$	$r_c(1-a) + r_e \frac{r_m + R_G}{r_e + r_b + R_G}$
CURRENT AMPLIFICATION A_i	$\frac{i_o}{i_i} = -\frac{-r_m + r_e}{r_c - r_m + r_e + R_L}$	$\frac{a}{1-a}$
POWER GAIN OG	$\frac{R_L(r_m - r_e)^2}{\left\{(r_c - r_m + r_e + R_L)\left[r_b(r_c - r_m + r_e + R_L) + r_e(r_c + R_L)\right]\right\}}$	$\frac{a^2 R_L}{(1-a)\left[r_e + r_b(1-a)\right]}$

CONDITIONS FOR APPROXIMATE FORMULAS:

$$r_b \ll r_c,\ r_e \ll R_L \ll (r_c - r_m),\ a = \frac{r_m}{r_c} \cong \alpha$$

Fig. 5—Common emitter stage formulas.

emitter connection than in the common base connection. There are many factors involved in this decrease in allowable applied potential, such as type of junction, the resistivity of the material on each side of the junction, and the current amplification factor. A rule of thumb commonly used is to apply a factor of 0.6 to arrive at the maximum allowable collector voltage for

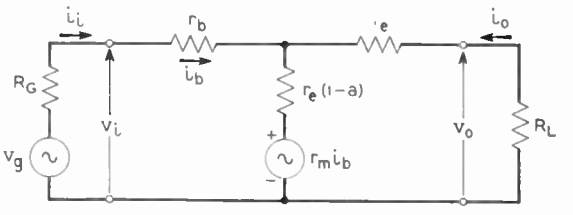

	EXACT	APPROXIMATE
INPUT RESISTANCE R_i	$r_b + r_c \frac{r_e + R_L}{r_c - r_m + r_e + R_L}$	$\frac{R_L}{1-a}$
OUTPUT RESISTANCE R_o	$r_e + \frac{(r_c - r_m)(r_b + R_G)}{r_b + r_c + R_G}$	$r_e + (r_b + R_G)(1-a)$
CURRENT AMPLIFICATION A_i	$\frac{i_o}{i_i} = \frac{-r_c}{r_c - r_m + r_e + R_L}$	$-\frac{1}{1-a}$
POWER GAIN OG	$\frac{r_c^2 R_L}{\left\{(r_c - r_m + r_e + R_L)\left[r_b(r_c - r_m + r_e + R_L) + r_c(r_e + R_L)\right]\right\}}$	$\frac{1}{1-a}$

CONDITIONS FOR APPROXIMATE FORMULAS:

$$r_b \ll r_c,\ r_e \ll R_L \ll r_c - r_m,\ R_G \ll r_c,\quad a = \frac{r_m}{r_c} \cong \alpha$$

Fig. 6—Common collector stage formulas.

the common emitter connection relative to that of the common base connection.

In the higher collector current regions, the characteristics may become excessively crowded, or for other types of units may actually become more widespread. Operation beyond a specified upper limit is subject to severe nonlinearity. It is therefore possible to delineate a bounded area of allowable operation. Excursions beyond these limits are subject to either excessive dissipations or to nonlinear distortion.

Paralleling the use made of static characteristics of electron tubes, output load lines can be drawn across the collector or output characteristics for dc and low-frequency studies. The quiescent point of operation and required biasing conditions may be determined from these plots. Indications of maximum undistorted signal performance may be obtained and point-by-point distortion studies facilitated. The effects of changing load resistance values and operating points can be rapidly evaluated by graphical means.[2]

Single-Stage Design Considerations

An amplifier may consist of a number of individual amplifier stages, coupled by passive networks. These networks should introduce minimum loss over the frequency band of interest. Expressions for the input and output resistances, current amplifications, and operating gains for individual stages in the three methods of connection have been dreived in the previous paper, and are shown in Figs. 4, 5, and 6 (above) for convenience.

A qualitative discussion of the variation of the input resistance R_i as a function of the load resistance R_L may be made on the basis of these formulas. For low values

of R_L less than $r_c(1-a)$, the input resistance of the common base and common emitter stage is small and relatively independent of the load for emitter currents of one mA or more. As the load resistance becomes larger, approaching the collector resistance r_c, both input resistances approximate the value r_e+r_b (~300 ohms). The input resistance of the common collector stage is also low for zero load resistance, but increases rapidly to values approximated by $R_L/(1-a)$. For large values of R_L greater than the collector resistance, the input resistance approaches r_c.

An examination of the variation of the current amplification A_i as a function of load resistance indicates that, for low values of R_L, the current amplifications approach the values a, $a/(1-a)$ and $1/(1-a)$, respectively. For values of load resistance between the limits $r_c(1-a)$ and r_c, the current amplification of both common emitter and common collector stages decreases rapidly, whereas only a small decrease is noted for the common base stage. These considerations will be useful in studying multistage amplifiers to aid in determining the method of connection which should be used in the various stages of the amplifier.

RC Coupling Networks

In RC-coupled junction transistor audio amplifier stages were it is usually desired to obtain large current amplification factors, the common emitter method of connection possesses several advantages. From ac considerations, the common emitter circuit will provide maximum power gain over wide ranges of terminating impedances.

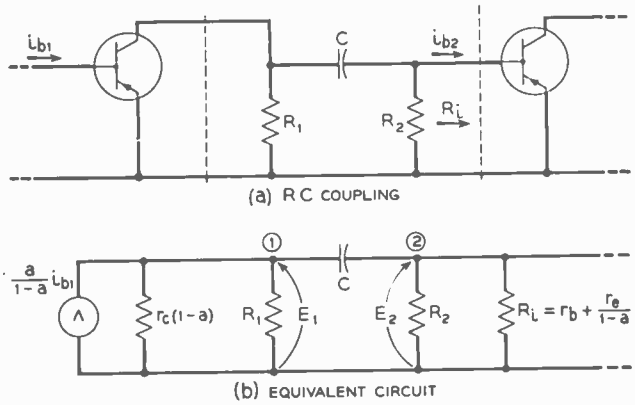

Fig. 7—RC coupling and equivalent circuit.

A simplified ac circuit for common emitter RC-coupled stages in shown in Fig. 7, together with an equivalent circuit. The loss introduced by the presence of the coupling elements is desired to be minimized. At midband, the impedance of the coupling capacitor C may be assumed negligible, and the resistor R_2 represents the total effective paralleling effect of all external biasing resistors connected to the base. The input resistance of the second stage may be approximated by

$$R_i \cong r_b + \frac{r_e}{1-} \cdot \tag{1}$$

If, by our assumptions,

$$R' = \frac{R_1 R_2}{R_1 + R_2}, \tag{2}$$

the current i_{b_2} introduced at the base of the second stage is related to the input current i_{b_1} by

$$i_{b_2} \cong \frac{a}{1-a}\left(\frac{R'}{R' + R_i}\right) i_{b_1}, \tag{3}$$

since the total bridging resistance R' will be small enough to justify using the approximate current amplification expression $A_i \cong a/(1-a)$. The above equation indicates the reduction in current amplification at midband resulting from the presence of the dc biasing resistors R_1 and R_2. Usual practice would require that $R' > 10R_i$, corresponding to a loss of approximately 0.8 db.

Below midband frequencies, the impedance of the coupling capacitor will introduce additional loss. Using the equivalent circuit shown in Fig. 7 and applying nodal analysis, an expression for the current gain may be derived:

$$A_i = \frac{i_{b_2}}{i_{b_1}} \cong \left[\frac{R_1 R_2 r_c a}{R_i + R_2(1-a)}\right] \cdot \left[\frac{1}{R_1 r_c(1-a) + \dfrac{R_1 + r_c(1-a)}{j\omega C}}\right] \tag{4}$$

The assumption has been made in deriving this equation that the input resistance of the second stage may be approximated by $r_b+r_e/(1-a)$. A 3-db reduction from the midband value of A_i will occur at the frequency specified by

$$\frac{1}{\omega C} = \frac{R_1 r_c(1-a)}{R_1 + r_c(1-a)} \tag{5}$$

A superior method of providing bias to the device having stabilization properties to be discussed in the section, Stabilization Techniques, is shown in Fig. 8, with equivalent circuits. At midband, the current amplification may be evaluated, assuming both coupling and by-pass capacitors to be perfect short circuits, and resistor $R_2 \gg Z_i$.

A Thevenin equivalent of the generator, its internal resistance and the collector load resistor R_1 may be derived:

$$Z_1 = \frac{r_c(1-a)R_1}{R_1 + r_c(1-a)}$$
$$v_g = \frac{R_1 r_m i_{b_1}}{R_1 + r_c(1-a)} \cdot \tag{6}$$

Similarly the impedance Z_2 may be approximated by

$$Z_2 \cong r_b + \frac{r_e}{1-a} \cdot \tag{7}$$

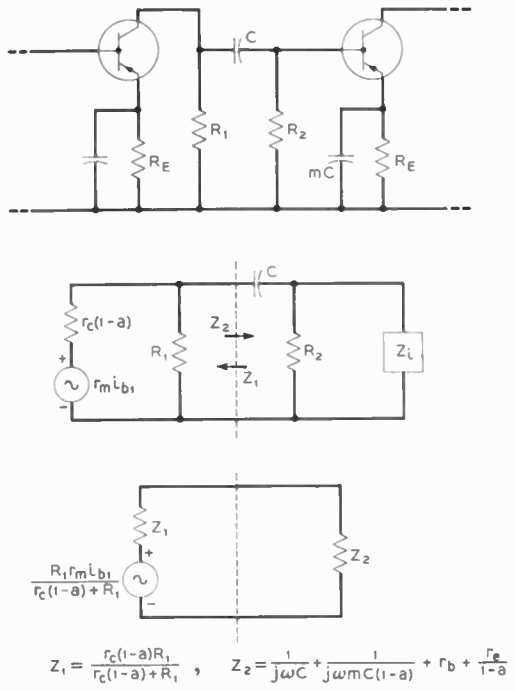

Fig. 8—RC coupling and equivalent circuits.

The current amplification at midband is

$$A_i \cong \frac{r_m R_1}{r_c(1-a)R_1 + [R_1 + r_c(1-a)]\left[r_b + \dfrac{r_e}{1-a}\right]} . \quad (8)$$

At the lower frequencies, the impedances of the coupling and by-pass capacitors must be considered. Assuming that $R_2 \gg Z_i$, the impedance Z_2 becomes:

$$Z_2 \cong \frac{1}{j\omega C} + \frac{1}{j\omega m C(1-a)} + r_b + \frac{r_e}{1-a} . \quad (9)$$

The low-frequency current amplification is

$$A_i \cong \frac{r_m R_1}{r_c(1-a)R_1 + [R_1 + r_c(1-a)]\left[\dfrac{1}{j\omega C} + \dfrac{1}{j\omega m C(1-a)} + r_b + \dfrac{r_e}{1-a}\right]} . \quad (10)$$

The one-half power lower corner frequency will occur when $|Z_1| = |Z_2|$, thus

$$\left|\frac{r_c(1-a)R_1}{R_1 + r_c(1-a)}\right| + \left|r_b + \frac{r_e}{1-a}\right| = \left|\frac{1}{j\omega C} + \frac{1}{j\omega m C(1-a)}\right| . \quad (11)$$

Solving for ω (3 db down)

$$\omega = \frac{1 + m(1-a)}{C(1-a)m\left[\dfrac{r_c(1-a)R_1}{R_1 + r_c(1-a)} + \left(r_b + \dfrac{r_e}{1-a}\right)\right]} . \quad (12)$$

For minimum effect of the capacitor shunting the emitter biasing resistor, obviously $m \to \infty$. A practical apportionment between the capacitor values may be obtained if $m = 1/(1-a)$, so that the effects of the coupling capacitor and shunting capacitor occur at the same frequency. The expression then reduces to

$$\omega(3 \text{ db down}) = \frac{2}{C\left[\dfrac{r_c(1-a)R_1}{R_1 + r_c(1-a)} + \left(r_b + \dfrac{r_e}{1-a}\right)\right]} . \quad (13)$$

The coupling capacitor C may be calculated, using (13), for a desired low-frequency stage response, and the emitter biasing capacitor determined by using $m = 1/(1-a)$.

Stabilization Techniques

One of the major problems confronting the designer of linear transistor amplifier circuits is the variation of the various parameters with temperature, operating point, and between units. The parameter of greatest importance in these respects is the collector current which flows with zero emitter current, usually designated $I_C(O, V_C)$ or simply I_{CO}. In junction-type units, the I_{CO} varies exponentially with temperature in accordance with the relationship[1,3]

$$I_{CO_2} = I_{CO_1} \epsilon^{0.08(T_2 - T_1)} \quad (14)$$

where

I_{CO_1}, I_{CO_2} are the equilibrium saturation currents due to minority carrier diffusion across the junction at temperatures T_1 and T_2, respectively.

T is temperature in °K.

The effects of variations in the I_{CO} of the transistor with temperature and between units must be compensated by correct design of the biasing arrangements, or marked departures from the desired quiescent operating point will be encountered.

The above considerations are pertinent to the design of the common emitter amplifier stage, as shown in Fig. 9, p. 149. The typical static output characteristics (V_C versus I_C with I_B as parameter) for the device at room temperature indicate that satisfactory linear operation about a quiescent operating point Q may be obtained. However, with increase in temperature, or with the use of a similar unit having a higher alpha, the static characteristics would be displaced to the right, as shown in dashed lines. Thus, any attempt to fix the operating point Q by supplying a constant base current is impractical. A current stabilizing method which has been widely used consists of a clamping voltage applied to the base and a constant emitter current supply which pro-

[3] G. L. Pearson and B. Sawyer, "Silicon P-N junction alloy diodes" Proc. IRE, vol. 40, p. 1348, November, 1952.

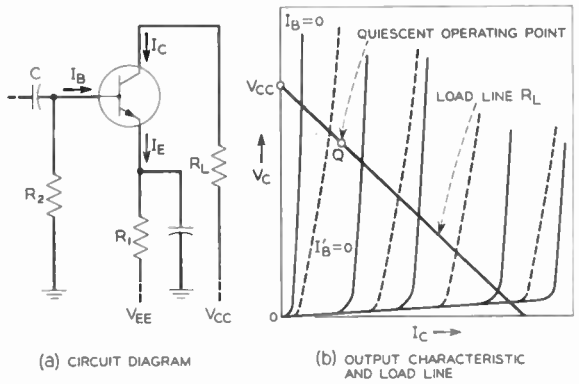

Fig. 9—Series biasing stabilization. (a) Circuit diagram. (b) Output characteristic and load line.

vides negative feedback at dc. The design is predicated upon a fixed emitter current, rather than a fixed base biasing current. An expression for the collector current may be derived in terms of the stabilizing elements R_1 and R_2, and the alpha of the device. The following assumptions may be made:

(a) The voltage V_{EB} developed from emitter to base may be neglected. For the majority of junction type units this voltage will be in the order of a few tenths of a volt.

(b) The collector to base voltage V_{CB} will be maintained within the operating region, where it has a negligible effect on the flow of collector current.

(c) The current amplification factor of a particular unit is constant over the operating range of interest.

The general expression[1,4] for the collector current in the common emitter connection is:

$$I_C = \frac{I_{CO}}{1-a} + \frac{aI_B}{1-a}. \tag{15}$$

By Kirchoff's current law, $\sum I_i = 0$, thus

$$I_E = I_C + I_B. \tag{16}$$

An expression for the base current I_B may now be obtained:

$$I_B = \frac{V_{EE} - I_C R_1}{R_1 + R_2}. \tag{17}$$

Substituting in (15),

$$I_C = \frac{(R_1 + R_2)I_{CO}}{R_1 + R_2(1-a)} + \frac{aV_{EE}}{R_1 + R_2(1-a)}. \tag{18}$$

The stabilizing effects become evident on examining the above equation. The large factor $1/(1-a)$ multiplying I_{CO} is replaced by the much smaller relationship

$$\frac{R_1 + R_2}{R_1 + R_2(1-a)}.$$

Other considerations come into play in determining the values of R_1 and R_2. The midband input impedance of the stage will be determined largely by

$$Z_i \cong r_b + \frac{r_e}{1-a}.$$

Thus, to avoid introducing excessive loss at midband,

$$R_2 \gg r_b + \frac{r_e}{1-a}. \tag{19}$$

An alternative method of obtaining bias stabilization has the form of a dc shunt negative feedback[5] as shown in Fig. 10, which is useful when a relatively high voltage

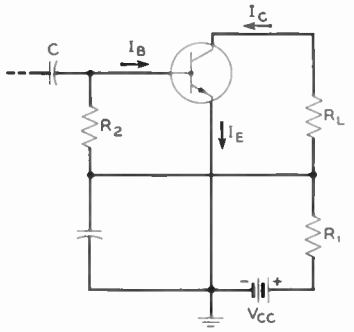

Fig. 10—Shunt biasing stabilization.

supply is available. It may be shown that the two forms of stabilization perform identically in providing stabilization of the dc operating point from variations in temperature and between units, and that (18) is valid for this circuit when V_{CC} is substituted for V_{EE}.

A somewhat similar method of connection[4] to obtain emitter biasing current and collector potential from the same battery is shown in Fig. 11, using a *p-n-p* junction

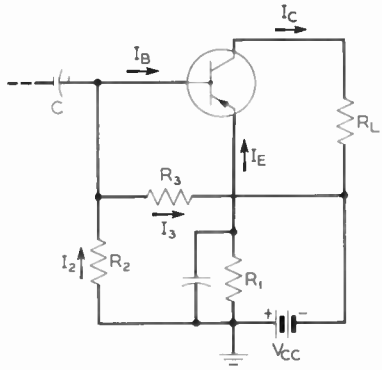

Fig. 11—Single battery bias stabilization.

transistor, as an example. For the same three basic assumptions, the following current relationships may be obtained:

$$I_B = I_2 - I_3 \tag{20}$$

$$I_C = I_B - I_E. \tag{21}$$

Also,

$$I_2 R_2 = I_E R_1 = V_{CC} - I_3 R_3 \tag{22}$$

$$I_C = \frac{I_{CO}}{1-a} - \frac{aI_B}{1-a}. \tag{23}$$

[4] R. F. Shea, Principles of Transistor Circuits," John Wiley and Sons, New York, 1953.

[5] This circuit concept is attributed to R. J. Kircher.

Solving these mesh relationships for I_C in terms of I_{CO} and the battery voltage V_{CC}:

$$I_C = \frac{(R_1R_2 + R_1R_3 + R_2R_3)}{R_1(R_2 + R_3) + R_2R_3(1 - a)} [I_{CO} + aV_{CC}R_2]. \quad (24)$$

To obtain stable operation, the factor multiplying I_{CO} should be as small as possible, consistent with maintaining a reasonable value of V_{CC} and power dissipation in the resistive elements. A desired operating collector-base voltage V_{CB} may be chosen from the static characteristics, consistent with assumption (b). This will result in a relationship between emitter and collector currents:

$$I_E = \frac{V_{CC} - I_CR_L - V_{CB}}{R_2}. \quad (25)$$

Also:

$$aI_E = I_C - I_{CO}. \quad (26)$$

Then:

$$R_1 = \frac{a}{I_C - I_{CO}} (V_{CC} - I_CR_L - V_{CB}) \quad (27)$$

$$R_3 = \frac{a(V_{CB} + R_LI_C)}{\frac{R_1}{R_2}(I_C - I_{CO}) + I_C(1 - a) - I_{CO}} \quad (28)$$

Using these equations, the resistance R_3 may be related to the stability multiplying factor (i.e., the factor multiplying I_{CO} in (24)).

$$\frac{R_1R_2 + R_1R_3 + R_2R_3}{R_1(R_2 + R_3) + R_2R_3(1 - a)} = \frac{R_3I_C + V_{CC}}{V_{CC} + R_3I_{CO}}. \quad (29)$$

The above relationships enable the stage to be completely designed. For any desired quiescent operating point, which implies that V_{CB}, I_C and load resistance R_L are known, as well as the I_{CO} and a of the transistor, a desired stability multiplying factor may be assumed. The resistor values R_1, R_2, and R_3 may then be calculated from the equations shown.

The dc power dissipated may be calculated by:

$$P_{DC} = V_{CC}(I_C + I_3) = \frac{V_{CC}(R_1 + R_2)}{2R_2} [I_C - I_{CO}]. \quad (30)$$

The shunt loss introduced by R_2 and R_3 must be considered from an over-all power gain standpoint. In order to realize desired output levels, it may be necessary to increase the stability multiplying factor.

Noise in Transistor Amplifiers

In the past, the noise power per cycle of junction-type devices varied inversely with the frequency over the audio range and up to a megacycle or more. In recent years, tremendous improvements in manufacturing processes and refinements in purification of the semiconductor materials has resulted in the commercial availability of junction-type transistors with extremely low noise figures.

Two different methods have been used to describe the noise properties of transistors.[6] One method is in terms of equivalent noise generators which may be introduced in the two-terminal pair representation of the device parameters. For linear circuit analysis,[7-9] this requires a suitable description of the power spectrum of two equivalent noise generators and a cross-spectrum between them.[10] The values ascribed to these equivalent generators will be functions of the dc biasing of the unit, but independent of the external circuit elements.

The second method makes use of a noise figure as a direct index of the noise characteristics of the device when used as an amplifier. The noise figure will be a function of the dc biasing conditions, frequency, and also of the signal generator impedance, but is independent of the load impedance. It is possible to calculate the noise figure of a device from the equivalent generator representation.

The equivalent generator method of describing the noise properties has been of use in device studies. However, for low-noise units where the noise levels are close enough to values which can be ascribed to uncorrelated thermal and shot noise sources,[11] the noise figure has been generally adopted as a more convenient and meaningful description of the device properties.

Noise Figure

The noise figure has been defined as the ratio of the total noise power in the output of an amplifier to that portion of the output noise resulting from thermal noise in the input generator resistance R_G. The noise figure provides a convenient basis for comparison of the noise properties of transistors. Representative values of noise figures measured at 1 kc for junction transistors designed for use in low-level stages are 4–20 db. The noise figure is a function of the dc biasing conditions, however, it has been verified[12] that noise arising in the emitter junction is almost independent of the collector voltage, whereas the noise due to the collector junction is highly dependent on the collector to base potential. Thus, for low noise operation, the junction transistors should desirably be biased at low collector voltages. One of the extremely useful characteristics of junction transistors

[6] E. Keonjian, and J. S. Schaffner, "Experimental investigation of transistor noise," Proc. IRE, vol. 40, pp. 1456–1461; November, 1952.

[7] H. C. Montgomery, "Transistor noise in circuit applications," Proc. IRE, vol. 40 pp. 1461–1472; November, 1952.

[8] P. M. Bargellini and M. B. Herscher, "Noise in audio amplifiers using transistors," Proc. IRE, vol. 43, pp. 217–227; February, 1955.

[9] E. A. Guillemin, "Communication Networks," vol. II, Chapter IV, John Wiley and Sons, New York, 1935.

[10] S. O. Rice, "Mathematical analysis of random noise," *Bell Sys. Tech. Jour.*, Vol. 23, pp. 283–332; July, 1944. And vol. 24, pp. 46–156; January, 1945.

[11] L. C. Pedersen, "Equivalent circuits of linear active four-terminal networks," *Bell Sys. Tech. Jour.*, vol. 27; October, 1948.

[12] H. C. Montgomery, "Electrical noise in semiconductors," *Bell Sys. Tech. Jour.*, vol. 31, pp. 950–975; September, 1952.

is the ability to provide high amplification factors,[1,13] at extremely low values of emitter current and collector potential.

Signal-to-Noise-Ratio

In the transistor amplifier stage shown in Fig. 12, it has been assumed that both the input signal generator impedance and the load impedance are pure resistances.

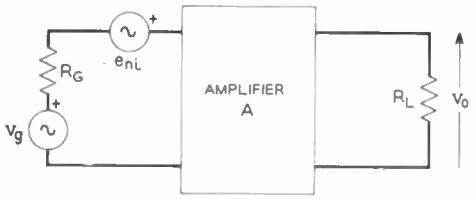

Fig. 12—Transistor amplifier-equivalent input noise source.

If thermal noise originating in the load resistance is neglected, the noise figure designated F' in the following analysis is the total noise power in the output divided by that portion of the noise power resulting from thermal noise in the generator resistance R_G. The mean-square value of the thermal noise voltage originating in R_G is

$$\bar{e}_n^2 = 4kTR_G(f_2 - f_1). \tag{31}$$

If the ratio of the output signal voltage to the input voltage v_0/v_g equals A, then the noise power in the output due to thermal noise in R_G is

$$P_{N'} = \frac{4kTR_G(f_2 - f_1)A^2}{R_L}. \tag{32}$$

If the total noise power in the output arises from a total noise voltage of mean-square value e_{n0}^2 developed across the load resistance R_L, then

$$P_{N\,(\text{total noise})} = \frac{\bar{e}_{n0}^2}{R_L}. \tag{33}$$

The noise figure F' may be expressed as

$$F' = \frac{P_N}{P_{N'}} = \frac{\bar{e}_{n0}^2}{4kTR_G(f_2 - f_1)A^2}. \tag{34}$$

It is desired to express the noise of the transistor amplifier in terms of an equivalent noise voltage generator in series with the input signal. Since this noise generator e_{ni} is to produce voltage e_{n0} across the load resistance R_G, the rms value of e_{ni} must be e_{n0}/A.

Substituting,

$$\bar{e}_{ni}^2 = 4kTR_G(f_2 - f_1)F' \tag{35}$$

The noise figure F is commonly expressed in terms of measurements made at 1,000 cps for a bandwidth of 1 cps. The noise spectrum over the audio-frequency range has been expressed as

$$dW = \frac{kdf}{f^n} \text{ noise power in watts/cycle.} \tag{36}$$

The exponent n has a value a little greater than unity, in the range 1.05–1.2. If the exponent n is assumed equal to unity, then the mean-square value of the noise voltage at the output is proportional to $n(f_2/f_1)$. Since the thermal noise in the output due to R_G is proportional to (f_2-f_1), the noise figure for an arbitrary bandwidth of (f_2-f_1) becomes:

$$F' = \frac{1000F \ln \dfrac{f_2}{f_1}}{f_2 - f_1}. \tag{37}$$

For a small bandwidth , such that

$$\frac{f_2}{f_1} \cong 1, \ln \frac{f_2}{f_1} = \frac{f_2 - f_1}{f_1}$$

and

$$F' \cong F\frac{1000}{f_1}. \tag{38}$$

The noise figure may be considered independent of the bandwidth, if the band remains relatively small. Substituting in (35)

$$\bar{e}_{ni}^2 = 4FkTR_G 1{,}000 \ln \frac{f_2}{f_1}. \tag{39}$$

Substituting numerical values and changing the base of the logarithmic term:

$$\bar{e}_{ni}^2 \cong 3.6 \times 10^{-17} R_G F \log \frac{f_2}{f_1} \text{ in volts}^2. \tag{40}$$

The available power at the input due to e_{ni}, defined as the power transferable to a matched load, is

$$P_{NI} = \frac{\bar{e}_{ni}^2}{4R_G} = 0.9 \times 10^{-17} F \log \frac{f_2}{f_1} \text{ in watts.} \tag{41}$$

Considering that for most amplifiers only the noise contributions of the first stage will be significant, the signal-to-noise ratio at the output of a transistor amplifier will then be equal to the ratio of the available signal power at the output to the available noise power:

$$\frac{S}{N} = \frac{\bar{v}_g^2}{4R_G P_{NI}} = \frac{\bar{v}_g^2}{3.6 \times 10^{-17} R_G F \log \dfrac{f_2}{f_1}}. \tag{42}$$

The maximum permissible noise figure requirements for a transistor to be used in the first stage of an amplifier may be determined from the above equation.

Transistor Parameters at Higher Frequencies

The description of the external behavior of the transistor at audio frequencies in terms of impedance, ad-

[13] R. L. Wallace, Jr. and W. J. Pietenpol, "Some circuit properties and applications of N-P-N transistors," *Bell Sys. Tech. Jour.*, vol. 30, pp. 530–563; July, 1951.

mittance and hybrid parameters has been covered in the previous paper.[1] At low frequencies, the equivalent circuit parameters are resistive and the current gain factor alpha is a real quantity. If resistive loads are employed, the input and output impedances are resistive, and voltage or current amplification and power gain calculations are therefore greatly simplified.

Prior to any discussion of feedback considerations and circuit configurations, the variations in the properties of the transistor at higher frequencies must be treated. The small-signal equations for frequencies of operation when the equivalent circuit elements include reactive effects are:

$$\begin{aligned} v_1 &= z_{11}i_1 + z_{12}i_2 \\ v_2 &= z_{21}i_1 + z_{22}i_2. \end{aligned} \tag{43}$$

In general, the z open-circuit impedance parameters are complex. In the low-frequency cases with which we have been concerned in the previous material, the static characteristics have given sufficient information to derive equivalent circuits, using the slopes of these curves, to evaluate resistive parameters, r_{11}, r_{12}, r_{21}, and r_{22}, which adequately described the behavior of the devices.

Many equivalent circuits have been derived to represent the behavior of the transistor at high frequencies.[4,14–16] In general, the more complete the representation, the more complex the equivalent circuit. The physical principles underlying some of the more important effects giving rise to the change in properties are:

1. *Transit Time*—The decreasing value of the amplification factor with increasing signal frequency may be attributed in part to the finite minority carrier transit time. If all of the carriers followed paths of equal length in traversing from emitter to collector and traveled at equal velocities, the equivalent current generator in the collector circuit would furnish a replica of the input signal, with a finite delay. Since the carriers follow unequal paths with a random distribution of velocities, they do not all arrive at the collector at the same time. This causes a smearing or dispersion effect, which results in a reduction in the amplitude and a phase shift. This degradation in frequency response becomes worse as the operating frequency is increased, until eventually there is no amplification.

2. *Collector Barrier Capacitance*—The barrier region, which is swept free of carriers by reason of the inverse potential, is a space-charge region. For the case of the alloy junction transistor, there is a rapid transition from base region to the collector region, the voltage across the barrier region is proportional to the square of the barrier thickness. The barrier charge increases with voltage and therefore possesses an intrinsic capacitance. The effective ac capacitance is inversely proportional to the square root of the barrier potential.

In the case of the grown junction transistor, where the transition from base to collector region is relatively gradual, the charge density is proportional to the distance away from the junction, and the barrier voltage is proportional to the cube of the barrier thickness. The effective capacitance is inversely proportional to the cube root of the barrier potential.

Since the collector to base operating potential is essentially concentrated across the barrier layer, the capacitance thus developed becomes of importance at higher frequencies.

3. *Emitter Barrier Capacitance*—The emitter barrier capacitance similarly limits the high-frequency response of the transistor. The effects of this reactive parameter are reduced if the source resistance is made as low as possible. Since the base resistance r_b is in series with the source in common base and common emitter connections, a good high frequency transistor should have a low base resistance. If the source impedance and base resistance are low, the upper frequency response limit is determined primarily by the collector junction capacitance and variation in the current gain due to the dispersion effect.

High-Frequency Equivalent Circuits

In general, an equivalent circuit should preferably be the simplest configuration which adequately represents the device behavior over the frequency band of interest. For comparison purposes and to facilitate design procedures, it should also have approximately the same form as the low-frequency representation.

In the frequency range below cut-off frequency of alpha,[17] equivalent circuits in Figs. 13–15, pp. 152, 153 will provide good approximations to transistor performance. The important modifications to the corresponding low-frequency equivalent circuits are the addition of the capacitor C_c across the collector resistance r_c, and the representation of z_m and alpha as complex quantities.

Additional factors, not evident from the circuits shown, are that r_e and C_c vary with frequency. The elements r_e and r_b are also frequency dependent, but to a much lesser degree, and are customarily assumed constant and resistive up to the cutoff frequency f_{a0}.

The variation of alpha with frequency is a function of the material properties and physical construction of the device. This function has been approximated by a low-pass RC network to derive an expression of the form:

$$a = \frac{a_0}{1 + j\dfrac{\omega}{\omega_{a0}}} \tag{44}$$

[14] L. J. Giacoletto, "Junction transistor equivalent circuits and vacuum tube analogy, PROC, IRE., vol. 40, pp. 1490–1493; November, 1952.

[15] R. L. Pritchard, "Frequency variations of junction transistor parameters," PROC. IRE, vol. 42, pp. 786–800; May, 1954.

[16] H. Statz, E. A. Guillemin, and R. A. Pucel, "Design considerations of junction transistors at higher frequencies," PROC. IRE, vol. 42, pp. 1620–1628; November, 1954.

[17] The alpha cutoff frequency f_{a0} has been defined as the frequency at which $|a|$ is 3 db below its low-frequency value a_0.

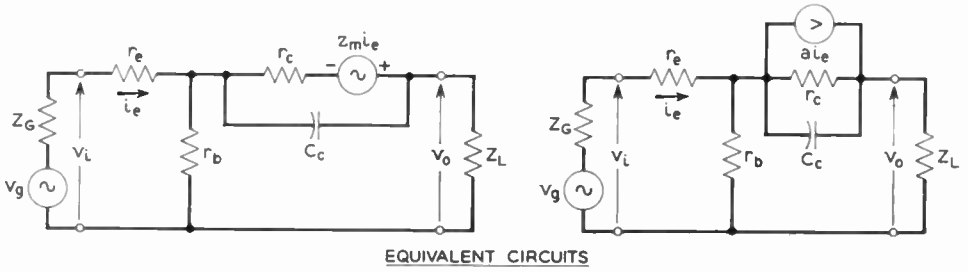

EQUIVALENT CIRCUITS

	EXACT	APPROXIMATE
INPUT IMPEDANCE Z_i	$r_e + r_b\left[\frac{z_c(1-a)\,Z_L}{r_b+z_c+Z_L}\right]$ WHERE $z_c = \frac{jX_c r_c}{r_c+X_c}$, $X_c = -\frac{1}{2\pi f C_c}$	$r_e + r_b\left[\frac{1-a+\frac{Z_L}{z_c}}{1+\frac{Z_L}{z_c}}\right]$ IF $r_b \ll z_c + Z_L$
OUTPUT IMPEDANCE Z_o	$z_c + r_b\left[\frac{r_e+Z_G-a z_c}{r_e+r_b+Z_G}\right]$	$z_c\left[\frac{r_e+Z_G+r_b(1-a)}{r_e+r_b+Z_G}\right]$ IF $r_b \ll z_c$, $Z_G = Z_i$
CURRENT AMPLIFICATION A_i	$-\frac{r_b(r_c+jX_c)+jX_c z_m}{r_b(r_c+jX_c)+jX_c r_c}$	$-\frac{z_m}{r_c} \Rightarrow a$ IF $r_b \ll \mathcal{R}e\left(\frac{jX_c z_m}{r_c+jX_c}\right) \ll \mathcal{R}e\left(\frac{jX_c r_c}{r_c+jX_c}\right)$
POWER GAIN OG	$\frac{\mathcal{R}e(Z_i)\,\lvert r_b+az_c\rvert^2}{\mathcal{R}e\left(r_e+r_b\left[\frac{z_c(1-a)+Z_L}{r_b+z_c+Z_L}\right]\right)\lvert Z_L+r_b+z_c\rvert^2}$	$\frac{(az_c)^2 R_L}{\mathcal{R}e\left(r_e+r_b\left[\frac{z_c(1-a)+R_L}{z_c+R_L}\right]\right)\lvert R_L+z_c\rvert^2}$ IF $Z_L=R_L$, $r_b \ll az_c$

Fig. 13—High-frequency equivalent circuits and formulas—common base connection.

where

a is the current gain at the operating frequency $f=\omega/2\pi$

a_0 is the low-frequency current gain

f_{a0} is the cutoff frequency of alpha, $f_{a0}=\omega_{a0}/2\pi$.

It has been mentioned that the parameters r_c and C_c vary with frequency. In order to obtain some idea of the magnitude of these variations for typical junction type transistors, they are plotted against a normalized frequency scale f/f_{a0} in Fig. 16, p. 154. Value of collector conductance g_c is plotted instead of r_c, and increases very abruptly in the neighborhood of the cutoff frequency. It is customary to neglect these effects for usual transistors in circuit analyses below the cutoff frequency. The collector capacitance exhibits a gradual decrease to approximately 75 per cent of its low-frequency value at the cutoff frequency.

If circuit analysis work is to be performed at frequencies in the region of and above the cutoff frequency of alpha, more complex equivalent circuits[18–20] must be used.

Common Base Amplifier Characteristics

The high-frequency equivalent circuit shown in Fig. 13 may be required in the design of audio-frequency circuits using large amounts of negative feedback. The analytical expressions for the input and output impedances, current amplification factor, and operating gain are as shown. These relationships are limited to analysis work below the cutoff frequency f_{a0}. It has been assumed that r_e and r_b are real quantities, constant with frequency.

Input Impedance—Z_i.

At the higher frequencies, where the phase angles of a and z_c must be considered, the approximate relation-

[18] Earl L. Steele, "Theory of Alpha for *pnp* diffused junction transistors," PROC. IRE, vol. 40, pp. 1424–1429; November, 1952.

[19] J. M. Early, "Effects of space charge layer widening in junction transistors," PROC. IRE, vol. 40, pp. 1401–1407; November, 1952.

[20] J. M. Early, "Design theory of junction transistors," *Bell Sys. Tech. Jour.*, vol. 32, pp. 1271–1312; November, 1953.

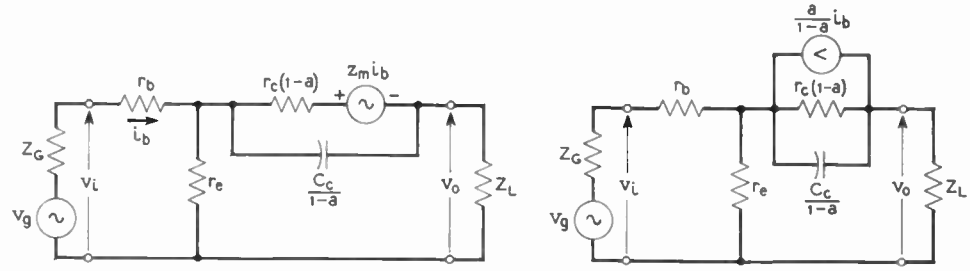

EQUIVALENT CIRCUITS

	EXACT	APPROXIMATE
INPUT IMPEDANCE Z_i	$r_b + r_e \left[\frac{z_c + Z_L}{r_e + Z_L + z_c (1-a)} \right]$	$r_b + r_e \left(\frac{1}{1-a} \right)$ IF $\lvert Z_L \rvert \ll \lvert z_c \rvert$, $r_e \ll Z_L + z_c (1-a)$
OUTPUT IMPEDANCE Z_o	$(1-a) z_c + r_e \left[\frac{r_b + Z_G + a z_c}{Z_G + r_b + r_e} \right]$	$(1-a) z_c$
CURRENT AMPLIFICATION A_i	$\frac{j x_c z_m - r_e (r_c + j x_c)}{r_e (j x_c + r_c) + j x_c (r_c - z_m)}$	$\frac{z_m}{r_c - z_m} = \frac{a}{1-a}$ IF $r_e \ll \mathrm{Re} \left[\frac{j x_c z_m}{r_c + j x_c} \right] \ll \mathrm{Re} \left[\frac{(r_c - r_m) j x_c}{r_c + j x_c} \right]$
POWER GAIN OG	$\frac{\mathrm{Re}(Z_L)}{\mathrm{Re}(Z_i)} \left\lvert \frac{a z_c - r_e}{r_e + z_c (1-a) + Z_L} \right\rvert^2$	$\frac{\mathrm{Re}(Z_L)}{\mathrm{Re}(Z_i)} \left\lvert \frac{a z_c}{Z_L + z_c (1-a)} \right\rvert^2$

Fig. 14—High-frequency equivalent circuits and formulas—common emitter connection.

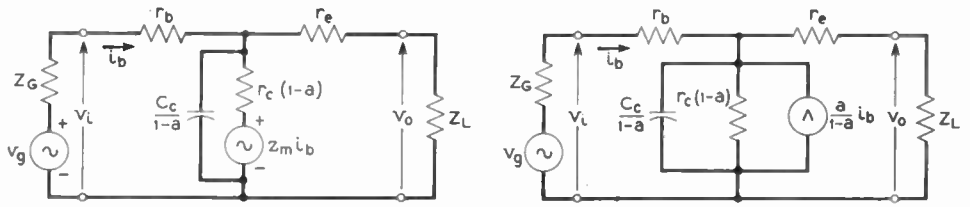

EQUIVALENT CIRCUITS

	EXACT	APPROXIMATE
INPUT IMPEDANCE Z_i	$r_b + z_c \left[\frac{r_e + Z_L}{r_e + z_c (1-a) + Z_L} \right]$	$\frac{r_b + r_e + Z_L}{1-a}$ IF $\frac{r_e}{z_c}, \frac{Z_L}{z_c} \ll (1-a)$
OUTPUT IMPEDANCE Z_o	$r_e + z_c (1-a) \left[\frac{r_b + Z_G}{r_b + z_c + Z_G} \right]$	$r_e + (r_b + Z_G)(1-a)$ IF $r_b, Z_G \ll z_c$
CURRENT AMPLIFICATION A_i	$\frac{-j x_c r_c}{r_e (r_c + j x_c) + (r_c - z_m) j x_c}$	$-\frac{r_c}{r_c - z_m} = \frac{-1}{1-a}$
POWER GAIN OG	$\frac{\mathrm{Re}\ Z_L}{\mathrm{Re}\ Z_i} \left\lvert \frac{1}{(1-a) + \frac{r_e}{z_c} + \frac{Z_L}{z_c}} \right\rvert^2$	$\frac{\mathrm{Re}\,(Z_L)}{\mathrm{Re}\,(Z_i)} \left\lvert \frac{1}{1-a} \right\rvert^2$ IF $\frac{r_e}{z_c}, \frac{Z_L}{z_c} \ll (1-a)$

Fig. 15—High-frequency equivalent circuits and formulas—common collector connection.

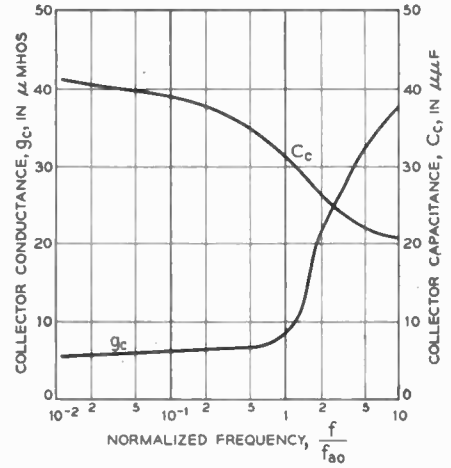

Fig. 16—Variation of C_c and g_c with normalized frequency.

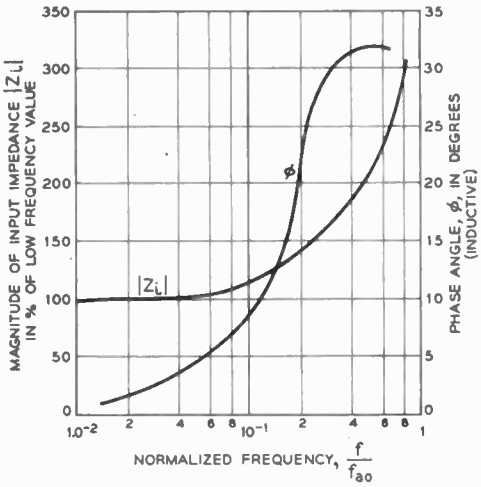

Fig. 17—Variation of input impedance with normalized frequency

ship

$$Z_i \cong r_e + r_b \left[\frac{1 - a + \frac{Z_L}{z_c}}{1 + \frac{Z_L}{z_c}} \right] \tag{45}$$

indicates that the fraction multiplying r_b will provide a positive imaginary term. Thus the input impedance will contain an inductive component. The magnitude of the input impedance increases with frequency to approach a value approximating r_e+r_b at f_{a0}, as illustrated in Fig. 17.

Output Impedance—Z_0.

The expression for the output impedance is

$$Z_0 \cong z_c \left[\frac{r_e + Z_G + r_b(1 - a)}{r_e + r_b + Z_G} \right]. \tag{46}$$

At lower frequencies, where z_c and a can be considered real numbers, this expression resolves to that given in the section on Single-Stage Design Considerations. The output impedance becomes capacitive for resistive loads in the frequency range when the phase angles of z_c and a affect the response, as shown in Fig. 18.

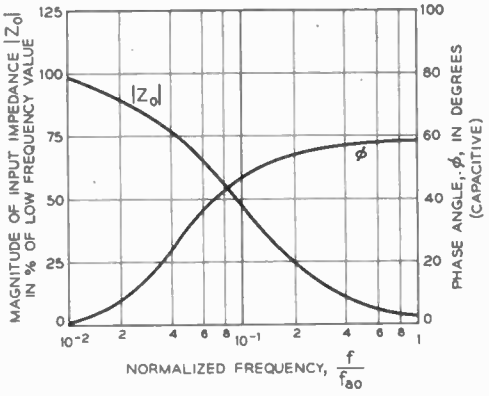

Fig. 18—Variation of output impedance with normalized frequency.

Power Gain

The approximate expression for the power gain on Fig. 13, assumed the load impedance to be resistive, so that $Z_L = R_L$.

$$OG \cong \frac{(az_c)^2 R_L}{\mathrm{Re}\left(r_e + r_b \left[\frac{z_c(1 - a) + R_L}{z_c + R_L} \right] \right) | R_L + z_c |^2}. \tag{47}$$

It is frequently useful to obtain a relationship between the high-frequency and low-frequency power gain. If the low-frequency power gain is G_0, at $(f/f_{a0}) \ll 1$, the ratio becomes

$$\frac{G}{G_0} \cong \frac{| az_c |^2 (R_L + r_c)^2 R_i}{| a_0 r_c |^2 (R_L + z_c)^2 \mathrm{Re}\,(Z_i)}. \tag{48}$$

The power gain may be down 3 db from its low-frequency value at only a few per cent of the f_{a0} of the device due to the variations of Re (Z_1) and z_c with frequency.

Common Emitter Amplifier Characteristics

The high-frequency equivalent circuits shown in Fig. 14 may be used to derive the expressions tabulated, using the general two-terminal pair relationships.

Current Amplification—A_i

The variation of the magnitude and phase of alpha with frequency has been described in a preceding section. The approximate expression for the current transmission of the stage, as shown on Fig. 14, is

$$A_i \cong \frac{-z_m}{r_c - z_m} \cong \frac{-a_0}{1 - a_0}. \tag{49}$$

The effect of the phase shift associated with alpha will result in a substantial decrease in the magnitude of A_i at frequencies for which alpha has not decreased appreciably from its low-frequency value. It may be shown[4] that the frequency at which the magnitude of A_i is down 3 db from its low-frequency value is of the order of $(1-a_0)f_{a0}$. Therefore, when a_0 is close to unity, the common emitter stage will have a very low cutoff frequency, even though the f_{a0} may be relatively high. This be-

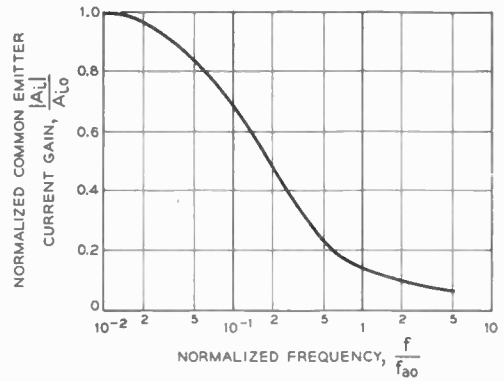

Fig. 19—Variation of normalized current gain factor versus normalized frequency.

havior is illustrated in Fig. 19. An alternative representation of the current gain of the common emitter stage, as derived in Appendix A, is

$$A_i \cong \frac{-a_0}{\left[1 - a_0 + \frac{Z_L + r_e}{r_c}\right] + j\omega\left[(Z_L + r_e)C_c + \frac{1}{\omega_{\alpha 0}}\frac{Z_L + r_e + r_c}{r_c}\right] - \frac{\omega^2 C_c(Z_L + r_e)}{\omega_{\alpha 0}}}. \quad (50)$$

If, in the above equation, the term

$$1 - a_0 + \frac{Z_L + r_e}{r_c}$$

in the denominator has a value less than 0.1 and therefore may be considered negligible, the current gain of the stage falls off at a rate of 6 db per octave, with a corner frequency specified by

$$\omega_{1(3\text{ db down})} = \frac{\omega_{\alpha 0}[Z_L + r_c + r_e(1 - a_0)]}{Z_L + r_e + r_c[1 + (Z_L + r_e)C_c\omega_{\alpha 0}]}. \quad (51)$$

A second 6 db per octave cutoff is introduced by the ω^2 term in the denominator of (50). The corner frequency of this second cutoff is given by

$$\omega_2 = \frac{r_c + Z_L + r_e + \omega_{\alpha 0} r_c C_c(Z_L + r_e)}{r_c C_c(Z_L + r_e)}. \quad (52)$$

In usual transistor amplifier circuits, this second cutoff frequency occurs in the region of the alpha cutoff frequency of the device. For this reason, the effects of the ω^2 term in (50) are commonly neglected in audio-frequency work.

Input Impedance—Z_i

The input impedance may be approximated by

$$Z_i \cong r_b + \frac{r_e}{1 - a}, \quad (53)$$

for the usual analysis purposes when the load impedance is much less than the collector impedance z_c. With increasing frequency, the input impedance decreases in magnitude, approaching the limiting value $r_b + r_e$. The exact expression tabulated also indicates that if the load impedance is resistive, the input impedance will be capacitive.

Output Impedance—Z_0

The output impedance may be approximated by

$$Z_0 \cong (1 - a)z_c + \frac{az_c r_e}{Z_G + r_b + r_e}. \quad (54)$$

The above expression assumes that $Z_G + r_b$ may be neglected in comparison with az_c. The magnitude of the output impedance then decreases with frequency to approximately 25 per cent of its low-frequency value at the cutoff frequency of alpha. If the generator impedance is comparable in magnitude to the input impedance of the stage, the phase angle of Z_0 will be capacitive, and proportional to the difference of the phase angles of $(1 - a)$ and z_c.

Power Gain

The power gain of the stage may be expressed as

$$OG \cong \frac{\text{Re}\,(Z_L)}{\text{Re}\,(Z_i)}\left|\frac{az_c}{Z_L + z_c(1 - a)}\right|^2. \quad (55)$$

If the load impedance Z_L is chosen to present a matched termination, in accordance with (54) the relationship becomes

$$OG \cong \frac{\text{Re}\,(Z_L)}{\text{Re}\,(Z_i)}\left|\frac{a}{2(1 - a)}\right|^2. \quad (56)$$

Consequently, the power gain cutoff frequency will be much lower than the $f_{\alpha 0}$ of the device.

Common Collector Amplifier Characteristics

The high-frequency equivalent circuits shown in Fig. 15 may be used to arrive at expressions defining the behavior of the common collector stage, under the limitations and assumptions discussed previously. Since the common collector stage is the only linear junction transistor configuration capable of possessing a high input impedance, together with the fact that it also has approximately unity voltage amplification, its operation and use is similar to the electron tube cathode-follower circuit. Unlike the cathode follower, the common collector stage is bilateral, capable of transmitting signals in either direction.[21] This discussion will be limited to considerations of transmission in only the forward direction.

[21] F. R. Stanzel, "Common collector transistor amplifier at carrier frequencies," Proc. IRE, vol. 41, pp. 1096–1102; September, 1953.

Input Impedance—Z_i

The input impedance may be calculated by

$$Z_i \cong r_b + \frac{r_e + Z_L}{1 - a}. \tag{57}$$

Since the load impedance appears in the numerator as the only independent variable, the input impedance is highly dependent upon Z_L. Expressions for the equivalent input conductance and capacitance have been derived[21] under the assumptions that the load admittance is represented by $G_L + j\omega C_L$, and that $r_e R \ll_L$

$$G_i \cong g_c + \frac{\left[1 - a_0 + \left(\frac{\omega}{\omega_{a0}}\right)^2\right] G_L}{1 + \left(\frac{\omega}{\omega_{a0}}\right)^2} - \frac{\omega_{a0} a_0 C_L \left(\frac{\omega}{\omega_{a0}}\right)^2}{1 + \left(\frac{\omega}{\omega_{a0}}\right)^2} \tag{58}$$

$$C_i \cong C_c + \frac{a_0 G_L}{\omega_{a0}\left[1 + \frac{\omega^2}{\omega_{a0}}\right]} + \frac{\left[1 - a_0 + \left(\frac{\omega}{\omega_{a0}}\right)^2\right] C_L}{1 + \left(\frac{\omega}{\omega_{a0}}\right)^2}. \tag{59}$$

The effect of the series r_b may be added to the above expressions, although this effect can generally be neglected.

A useful set of approximate values can be obtained by assuming that the $(\omega/\omega_{a0})^2$ term may be neglected. These approximations have been found valid up to about 0.1 of the cutoff frequency.

$$G_i \cong g_c + (1 - a_0) G_L - \omega_{a0} C_L a_0 \left(\frac{\omega}{\omega_{a0}}\right)^2 \tag{60}$$

$$C_i \cong C_c + \frac{a_0 G_L}{\omega_{a0}} + (1 - a_0) C_L. \tag{61}$$

These equations show that at low frequencies both input conductance and capacitance are nearly independent of frequency. By maintaining C_L at low values, the frequency dependence can be made small up to $0.1\, f_{a0}$.

The input resistance increases as the load resistance is increased, with an upper limit of r_c as determined by the first term in (60). The capacitive component is decreased as the load resistance is increased, approaching C_c as a lower limit.

Output Impedance—Z_0

Generalized expressions for the output conductance and capacitance may be obtained in the same manner. The assumption is made that the source is represented by $G_G + j\omega C_G$, and that $r_b \ll R_G$.

$$G_0 \cong \frac{\left[1 - a_0 + \left(\frac{\omega}{\omega_{a0}}\right)^2\right] g_c}{(1 - a_0)^2 + \left(\frac{\omega}{\omega_{a0}}\right)^2} + \frac{\left[1 - a_0 + \left(\frac{\omega}{\omega_{a0}}\right)^2\right] G_G}{(1 - a_0)^2 + \left(\frac{\omega}{\omega_{a0}}\right)^2} + \frac{\omega_{a0}\left(\frac{\omega}{\omega_{a0}}\right)^2 a_0 (C_c + C_G)}{(1 - a_0)^2 + \left(\frac{\omega}{\omega_{a0}}\right)^2} \tag{62}$$

$$C_0 \cong \frac{\left[1 - a_0 + \left(\frac{\omega}{\omega_{a0}}\right)^2\right](C_c + C_G)}{(1 - a_0)^2 + \left(\frac{\omega}{\omega_{a0}}\right)^2} - \frac{a_0 g_c}{\omega_{a0}\left[(1 - a_0)^2 + \left(\frac{\omega}{\omega_{a0}}\right)^2\right]} - \frac{a_0 G_G}{\omega_{a0}\left[(1 - a_0)^2 + \left(\frac{\omega}{\omega_{a0}}\right)^2\right]}. \tag{63}$$

The effect of the series r_e may be added to the above expressions for completeness. Since the resistive component of the output impedance is fairly low, it is often necessary to consider the effect of this series element. The output resistance is low and increases quite markedly with frequency at low frequencies. As the frequency increases, the output resistance approaches an asymptotic value of essentially R_G for low values of R_G. For higher values of R_G, the asymptotic value is reduced in value by the presence of the other two resistive components of (62).

The output capacitance is negative for low frequencies and approaches zero as frequency is increased.

Current and Voltage Transmission Ratios

These ratios may be found by solving the mesh equations for the equivalent circuits shown in Fig. 15.

$$\frac{v_0}{v_i} \cong \frac{r_c R_L}{(r_c + r_b)[R_L + r_b(1 - a) + r_e]} \tag{64}$$

$$\frac{i_0}{i_i} \cong \frac{-r_c}{(r_b + r_c)(1 - a) + (R_L + r_e)} \cong -\left[\frac{1}{1 - a} + \frac{r_c}{R_L}\right]. \tag{65}$$

For larger values of R_L, the voltage ratio approaches unity.

Transistor Feedback Amplifiers

Feedback principles have been applied in the field of electron-tube amplifier design to achieve many desirable characteristics. When feedback is used, the effective linearity of the amplifier is greatly increased, and the amplifier gain is stabilized against variations in both the parameters of the active devices and the passive components. Feedback may be used to control the input and output impedances of an amplifier, and in addition, noise originating in the later stages of amplification, such as power supply hum, is reduced.

The use of feedback also has its disadvantages. Additional stages of amplification are usually required, and a stability problem is introduced which may substantially increase the design complexity. The application of degenerative feedback to transistor amplifiers

involves many of the same considerations present in the design of comparable electron tube amplifiers.

The Feedback Equations

The feedback amplifier, in its simplest form, may be regarded as the combination of an ordinary amplification circuit and a feedback network or β circuit, by means of which a portion of the output of the amplification circuit may be returned to the input. Considering both amplification and feedback circuits as two-terminal pair networks, the elementary configuration shown in Fig. 20 may be drawn.

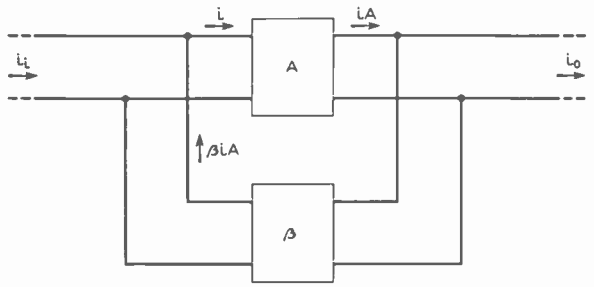

Fig. 20—Basic feedback configuration.

β may be defined as the percentage of the output current of the amplifier that is fed back to the input of the amplifier. The forward current transfer ratio A_i may be established as

$$A_i = \frac{i_0}{i_1} = \frac{A(1-\beta)}{1-A\beta} \cdot \tag{66}$$

This may be placed in the form

$$A_i = \frac{A\beta}{1-A\beta} \frac{(1-\beta)}{\beta} \cdot \tag{67}$$

For high-gain amplifiers with large amounts of feedback, the feedback factor $A\beta$ is much greater than unity and the current ratio A_i becomes

$$A_i \cong \frac{1-\beta}{\beta} \cdot \tag{68}$$

The current ratio is then determined primarily by the transmission through the feedback circuit. The error in this conclusion due to the departure of $|A\beta/(1-A\beta)|$ from unity is generally termed the $A\beta$ effect or $A\beta$ error.

Stability Criterion

In deriving the above equations, it was assumed that when the feedback connections were made the combination of amplifier and β network remained free from spontaneous oscillations. Equation (66) shows that the current ratio A_i with feedback is potentially infinite for any frequency which causes the feedback factor $A\beta$ to have the value $(1+j0)$; the possibility of a large free-response exists.

The stability criterion for single loop feedback amplifiers may be based on $1-A\beta$, in a manner analogous to Nyquist's criterion tube amplifiers. The stability of any amplifier may be investigated by the following procedure:

(1) The complex values of the feedback factor $A\beta$ at real frequencies from zero to infinity are determined.

(2) The locus of the points $A\beta$ are plotted in the complex plane, as frequency is varied from zero to infinity. If $A\beta$ is zero for zero frequency as well as infinity, this is a closed curve. If $A\beta$ is not zero for zero frequency, as in the case of dc amplifiers, a closed curve may be obtained by plotting a mirror image of the real frequency curve.

(3) If the closed curve obtained does not enclose the point $(1+j0)$, the circuit will be stable when the feedback path is closed.

Effect of Variations in the Active Elements

The equations characterizing the effects of feedback in stabilizing the forward transmission of the amplifier against variations in the elements making up the current gain section of the amplifier may be developed. If the current amplification factor A should change for some reason, such as aging of the transistors or variations in the power supply, the effect on the overall current ratio A_i may be determined.

Equation (66) may be differentiated to obtain

$$dA_i = dA \frac{(1-\beta)}{(1-A\beta)^2} \cdot \tag{69}$$

Dividing by (66),

$$\frac{dA_i}{A_i} = \frac{dA}{A} \frac{(1)}{(1-A\beta)} \cdot \tag{70}$$

Thus relative changes in the current amplification are decreased by the factor $1/(1-A\beta)$ with the application of degenerative feedback. In a similar fashion, reductions in the noise and distortion arising within the current amplification stages of the amplifier will result.

It should not be assumed that a feedback amplifier always has a noise advantage, as compared to an amplifier without feedback having the same current amplification. The use of feedback does not permit the design of an amplifier using a transistor with a poorer noise figure in the input stage. Unless the feedback action permits the adjustment of the input impedance of the amplifier without the necessity of employing a dissipative terminating resistor, it is ineffective in reducing the noise contributions of the input circuitry. The same care must be taken in the design of the first stage of a feedback amplifier from a noise, distortion and hum viewpoint, as is required for an amplifier without feedback.

Impedance of an Active Circuit

In any network, the impedance at any frequency between any two points of the net may be defined as the

ratio of the ac potential difference maintained across the points by an external emf, to the resulting current flowing between the points. Impedance may be determined, therefore, in terms of a response to an applied excitation signal. If the network contains active elements and there is feedback present, the resultant current may be due in part to the excitation of the active elements, since an amplified component may be returned via the feedback path.

A general relationship has been derived pertaining to the effect which feedback may have upon the impedance measured between any two points in a feedback network. It is assumed that the impedance which would be obtained in the absence of feedback may be determined by ordinary circuit analysis or measurement. The relationship is thus primarily concerned with the modification produced in the known passive impedance by the addition of feedback.

$$Z_F = Z_F{}^0 \frac{1 - (A\beta)_0}{1 - (AB)_\infty} \tag{71}$$

where

Z_F is the impedance between any two points of a closed single loop feedback system.

$Z_F{}^0$ is the impedance between these two points[22] without feedback.

$(A\beta)_0$ is the $A\beta$ of the feedback system with the two terminals defining Z_F short-circuited (zero impedance).

$(A\beta)_\infty$ is the $A\beta$ of the feedback system with the two terminals defining Z_F open-circuited (infinite impedance).

If the analysis methods are based upon the admittance concept, the relationship becomes

$$Y_F = Y_F{}^0 \frac{1 - (A\beta)_0}{1 - (A\beta)_\infty}, \tag{72}$$

where

Y_F is the admittance between any two points of a closed single loop feedback system.

$Y_F{}^0$ is the admittance between these two points in the absence of feedback.

$(A\beta)_0$ is the $A\beta$ of the feedback system with the two terminals defining Y_F open-circuited (zero admittance).

[22] This so-called "passive" impedance $Z_F{}^0$ may be thought of as the value the impedance Z_F assumes as the amplification A approaches zero, and the remaining properties and passive impedance relationships of the $A\beta$ loop are not altered. This concept, due to H. S. Black, permits analytical evaluations of $Z_F{}^0$ to be made by assuming that the active devices are deactivated by some means. In electron tubes, this may be accomplished by turning off the heater supply. This definition of $Z_F{}^0$ may be applied relative to the equivalent circuits shown in Fig. 14 for a common emitter connected transistor as an example. Thus, in order to calculate $Z_F{}^0$, it may be assumed that the current contributions of the equivalent circuit current generator (or voltage contributions, if the voltage generator representation is used) approach zero. The effects of alpha on the bilateral equivalent circuit passive elements must be retained in computing $Z_F{}^0$. Thus, for example, the equivalent collector resistance would remain as $r_c(1-a)$.

$(A\beta)_\infty$ is the $A\beta$ of the feedback system with the two terminals defining Y_F short-circuited (infinite admittance).

These equations describe the effects of the feedback on the impedance or admittance of feedback amplifiers. Specific examples will serve to make more apparent the usefulness of these relationships.

Input Impedance with Series Feedback

In a common emitter transistor amplifier, an external resistance may be placed in series with the emitter to afford series type negative feedback, as shown in Fig. 21. The mesh X-Y-W has been introduced in the equivalent circuit, with Y-W and W-X being short-circuited, and X-Y connected with an infinite impedance current generator. This generator will be considered as an external unit current source applied at the collector junction to activate the circuit during the $A\beta$ evaluations.

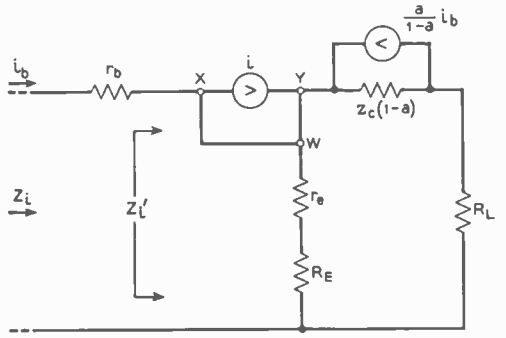

Fig. 21—Common emitter amplifier—series feedback.

Passive impedance across input terminals without feedback may be evaluated, assuming $a/1-a)i_b \to 0$ and the external unit current source deactivated:

$$Z_i{}^0 = r_b + \frac{(r_e + R_E)[z_c(1-a) + R_L]}{r_e + R_E + z_c(1-a) + R_L}. \tag{73}$$

Since r_b is a simple series resistance adding linearly to the input impedance, it facilitates the analysis to consider the input impedance Z_i' at the node X. Thus

$$Z_i' = \frac{(r_e + R_E)[z_c(1-a) + R_L]}{r_e + R_E + z_c(1-a) + R_L}. \tag{74}$$

It is now necessary to evaluate the A of the feedback system, under the conditions specified by (71). The equivalent circuit current generator is considered activated, and a unit current generator is inserted between points X and Y. The evaluation of A may be made by considering the return current to the point X via the path W-X as shown in Fig. 22.

(a) With point X short-circuited to the ground node to determine $(A\beta)_0$.

The unit current results in a current $a/(1-a)$ being developed by the equivalent circuit current generator. This current will be divided inversely proportional to the impedances of the two branch paths available. That

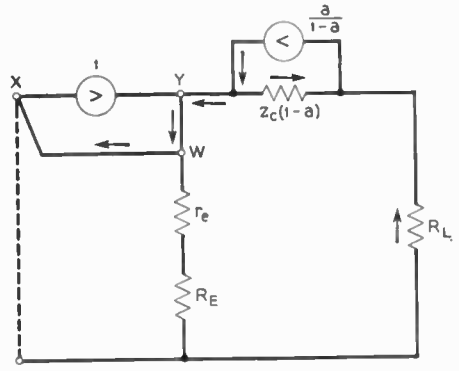

Fig. 22—*AB* evaluation.

portion flowing through the return path *W-X* will be

$$(A\beta)_0 = -\left[\frac{a}{1-a}\right]\frac{z_c(1-a)}{R_L + z_c(1-a)}. \tag{75}$$

The minus sign signifies that the feedback is degenerative. Then

$$1 - (A\beta)_0 = \frac{R_L + z_c(1-a) + az_c}{R_L + z_c(1-a)}. \tag{76}$$

(b) With point *X* open-circuited to determine $(A\beta)_\infty$.

The unit current generator, referring to Fig. 22, is assumed to be of infinite internal impedance, and none of the current $a/(1-a)$ developed by the equivalent circuit current generator will pass through the return path *W-X*, thus $(A\beta)_\infty = 0$. Then

$$1 - (A\beta)_\infty = 1. \tag{77}$$

The input impedance Z_i' may now be evaluated. From (71):

$$Z_i' = Z_i'^0[1 - (A\beta)_0]. \tag{78}$$

Substituting:

$$Z_i' = \frac{(r_e + R_E)(z_c + R_L)}{r_e + R_E + z_c(1-a) + R_L}. \tag{79}$$

Therefore,

$$Z_i = r_b + \frac{(r_e + R_E)(z_c + R_L)}{r_e + R_E + z_c(1-a) + R_L}. \tag{80}$$

This relationship could, of course, have been obtained in a more direct manner using the equation for the input impedance on Fig. 14 and substituting $(r_e + R_E)$ for r_e.

Input Impedance with Shunt Feedback

The effect of shunt feedback applied from collector to base on the input impedance of a common emitter stage may be evaluated using the equivalent circuit shown in Fig. 23, and the detailed analysis procedures

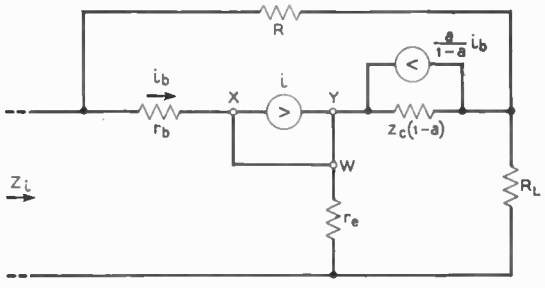

Fig. 23—Common emitter amplifier—shunt feedback.

of Appendix B. The input impedance expression derived is

$$Z_i = \frac{R_L R(r_e + r_b) + (R_L + R)[r_e r_b + z_c(r_e + r_b(1-a))]}{r_e r_b + z_c[r_e + r_b(1-a)] + R_L(r_b + z_c + R) + R[r_e + z_c(1-a)]}. \tag{81}$$

These two examples illustrate that series negative feedback may be used to magnify the input impedance of amplifiers, and shunt feedback may be applied in such a manner as to reduce the input impedance, in exactly the same fashion as in electron tube amplifiers.

APPENDIX A

Common Emitter Amplifier Stage-Current Gain

(This derivation is attributed to F. H. Blecher.)

The current gain expression for the amplifier stage whose equivalent circuit is shown in Fig. 14 may be determined, under the assumptions that

(a) r_e and r_b are resistive and constant over the frequency band of interest,

(b) $r_e \ll Z_G + r_b$,

(c) the frequency variation of alpha is given by

$$a = \frac{a_0}{1 + j\dfrac{\omega}{\omega_{a0}}}.$$

Using mesh analysis, the current flowing in the output circuit may be written as

$$I_0 \cong \frac{\left[\dfrac{r_e}{r_c(1-a)}(1 + j\omega r_c C_c) - \dfrac{a}{1-a}\right]v_g}{\dfrac{Z_L + r_e}{r(1-a)}(Z_G + r_b)(1 + j\omega r_c C_c) + (Z_G + r_b) + \dfrac{a}{1-a}r_e}. \tag{82}$$

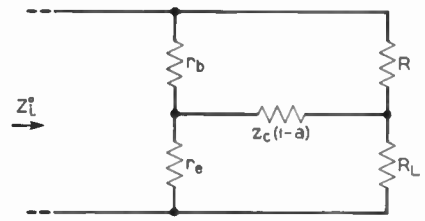

Fig. 24—Z_1^0 evaluation-equivalent passive network,

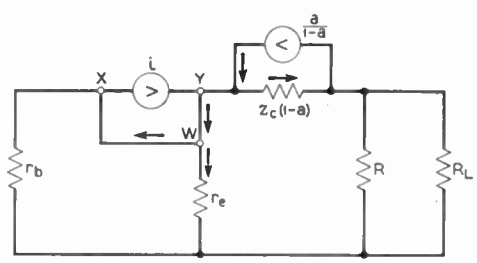

Fig. 25—$(AB)_\infty$ evaluation.

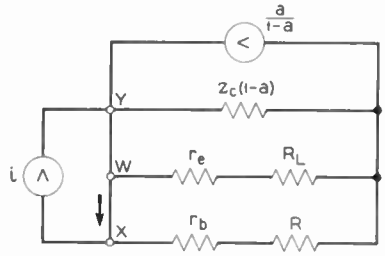

Fig. 26—$(AB)_0$ evaluation.

For usual transistors, operating in the frequency range below the f_{a0} of the device, the first term in the numerator will at least be an order of magnitude less than the second term. Substituting the expression for the frequency variation of alpha in (82), and neglecting the first term in the numerator:

$$I_0 \cong \frac{\dfrac{-r_c a_0 v_g}{(Z_L + r_e)(Z_G + r_b)}}{1 + \dfrac{r_c}{Z_L + r_e}(1 - a_0) + \dfrac{a_0 r_e r_c}{(Z_L + r_e)(Z_G + r_b)} + j\omega\left[r_c C_c + \dfrac{1}{\omega_{a0}} \dfrac{r_c}{(Z_L + r_e)} \dfrac{1}{(\omega_{a0})}\right] - \dfrac{\omega^2 r_c C_c}{\omega_{a0}}} . \quad (83)$$

Assuming a constant current source at the input, the current gain A_i may be expressed as:

$$A_i = \frac{I_0}{I_i} \cong \frac{-a_0}{\left[1 - a_0 + \dfrac{Z_L + r_e}{r_c}\right] + j\omega\left[(Z_L + r_e)C_c + \dfrac{1}{\omega_{a0}}\left(\dfrac{Z_L + r_e + r_c}{r_c}\right)\right] - \dfrac{\omega^2 C_c (Z_L + r_e)}{\omega_{a0}}} . \quad (84)$$

APPENDIX B

Input Impedance with Shunt Feedback

The equivalent circuit of a common emitter amplifier stage with shunt feedback applied from collector to base is shown in Fig. 23.

Passive Impedance Z_i^0

In the determination of the passive impedance Z_i^0 the equivalent circuit current generator $a/(1-a)i_b$ and the unit current generator are assumed equal to zero. The circuit may be represented by the passive bridge network shown in Fig. 24. Then

$$Z_i^0 = \frac{RR_L(r_e + r_b) + r_e r_b(R + R_L) + z_c(1 - a)(r_e + r_b)(R + R_L)}{(r_e + R_L)(r_b + R) + z_c(1 - a)(r_e + r_b + R + R_L)} . \quad (85)$$

Short-Circuit $(1 - A\beta_0)$

The equivalent circuit current generator is considered reactivated, and a unit current generator inserted between points X and Y. With the input node shorted to ground, the configuration becomes that shown in Fig. 25. Equivalent circuit generator furnishes $a/1-a)$ units of current in response to the unit current. That portion flowing in the path W-X is the return current to be found. The $A\beta_0$ is

$$(A\beta)_0 = -\left(\frac{a}{1 - a}\right)\frac{r_e}{r_b + r_e}\left[\frac{z_c(1 - a)}{\dfrac{r_e r_b}{r_e + r_b} + \dfrac{R_L R}{R_L + R} + z_c(1 - a)}\right] . \quad (86)$$

The return difference $1 - A\beta_0$ may be evaluated by

$$1 - (A\beta)_0 = \frac{r_e r_b(R_L + R) + R_L R(r_e + r_b) + z_c(R_L + R)[r_e + r_b(1 - a)]}{r_e r_b(R_L + R) + R_L R(r_e + r_b) + z_c(1 - a)(r_e + r_b)(R_L + R)} . \quad (87)$$

Open-Circuit $(1-A\beta_\infty)$

The input node is open-circuited, and the equivalent circuit resolves to that shown in Fig. 26 on opposite page.

The $(A\beta)_\infty$ will be equal to the return current flowing in the path W-X, through the series combination of $(R+r_b)$. The current furnished by the equivalent circuit generator will divide in proportion to the admittances of the three paralleling branches.

$$(A\beta)_\infty = -\frac{a}{1-a}\left[\frac{\dfrac{1}{R+r_b}}{\dfrac{1}{R+r_b}+\dfrac{1}{z_c(1-a)}+\dfrac{1}{R_L+r_e}}\right]. \quad (88)$$

Thus,

$$1-(A\beta)_\infty = \frac{z_c(R_L+r_e)+(r_b+R)(R_L+r_e)+(r_b+R)z_c(1-a)}{z_c(1-a)[R_L+r_e+r_b+R]+(r_b+R)(R_L+r_e)}. \quad (89)$$

Input Impedance

The input impedance with shunt feedback may be derived by using the general impedance relationship

$$Z_F = Z_F{}^0\frac{1-A\beta_0}{1-A\beta_\infty}. \quad (90)$$

Substituting,

$$Z_i = \frac{R_LR(r_e+r_b)+(R_L+R)[r_er_b+z_c(r_e+r_b(1-a))]}{r_er_b+z_c[r_e+r_b(1-a)]+R_L(r_b+z_c+R)+R[r_e+z_c(1-a)]}. \quad (91)$$

Analyses of Drivers for Single-Ended Push-Pull Stage*

HIROSHI AMEMIYA†

Push-pull stages require two opposite-phase driving voltages of the same amplitude. In conventional push-pull amplifiers, this is not a problem. In single-ended push-pull amplifiers, however, this requirement limits the types of usable drivers because of the apparently unbalanced structure of the push-pull stage. Four possible drivers, namely, the split-load phase inverter driver, the cathode-coupled phase inverter driver, the extended cathode-coupled phase inverter driver, and the Coulter driver, are analyzed with stress on the balance of the driving voltages.

A FEW YEARS ago, the application of a single-ended push-pull circuit to audio amplifiers was suggested by Peterson and Sinclair.[1] Fig. 1 shows the basic circuit of the single-ended push-pull connection, where the two output tubes are terminated in the common load impedance Z. Although the plate supply

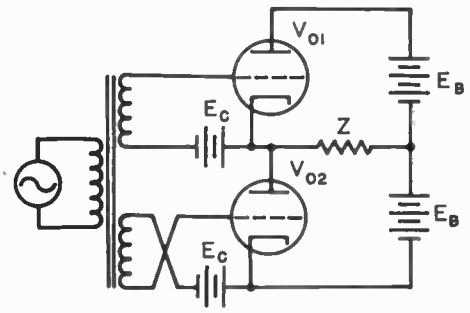

Fig. 1—The basic circuit of the single-ended push-pull amplifiers.

voltage is twice the normal value with this circuit arrangement, the output transformer may be eliminated entirely. When a high plate supply voltage is not feasible, the connection of Fig. 2 may be used, employing an output transformer with separate primary windings.

In conventional push-pull circuits, two output tubes are coupled through the output transformer, and the

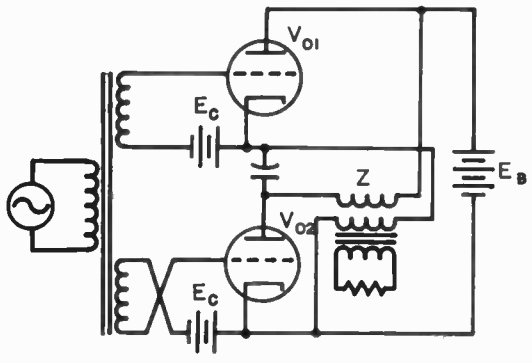

Fig. 2—A single-ended push-pull amplifier with a driving transformer.

leakage inductance between the two primary windings causes serious switching transients at high frequencies in class -AB and -B amplifiers. On the other hand, in the single-ended push-pull circuit the output tubes work into the same load, and switching transients are eliminated completely.

Except for the output connection, the single-ended push-pull circuit is identical with the conventional push-pull circuit, thus enjoying the advantages of the push-pull connection. The driving voltages for the output tubes must be of the same magnitude and of opposite phase. This condition is easily satisfied by using a driving transformer, as shown in Figs. 1 and 2. The driving transformer should, however, be avoided because of its cost and poor characteristics at extreme frequencies. Usually the negative side of the plate voltage supply is grounded; in other words, the cathode of the lower output tube V_{02} is at the ground potential and that of the upper tube V_{01} is at the output voltage. This unbalance complicates the problem of driving. The requirements for the driving voltages are:

1. Driving voltages between the grid and the cathode of the output tubes are equal in magnitude and opposite in phase.
2. The above condition is not affected by the variation of the load impedance Z of the output stage.

The first condition is an obvious one. In single-ended push-pull amplifiers the output voltage across Z exerts influence on the driver stage unless a driving transformer is used, and this is why the second condition is important. The impedance of the load, for instance, a loudspeaker, varies considerably with frequency, and if balance of the driving voltages is destroyed by load impedance variation, amplifier isn't a push-pull amplifier.

In order to supply balanced driving voltages to the unbalanced push-pull stage, satisfactory drivers have unbalanced construction. In the analyses presented here the effects of stray and inter-electrode capacities are neglected and the linearity of circuit elements is assumed. It is also assumed that the output impedance of the amplifier, which is the impedance of the plate resistances of the output tubes and the load impedance Z connected in parallel, is very low. This is justified, since power tubes are generally used for output tubes.

Split-Load Phase Inverter Driver

The split-load phase inverter driver has two equal load resistors, one in the plate and the other in the cathode. Figs. 3–6 are single-ended push-pull amplifiers, with the split-load phase inverter driver. These are equivalent signal-voltage circuits in which all the direct-current components have been omitted. V_{01} and V_{02} are the output tubes, and V_1 is the driver. It is to be noted that one of the load resistors of V_1 is returned

* Original manuscript received by the IRE, May 6, 1955. Revised manuscript received June 3, 1955.

† Electrical Engineering Department, University of Tokyo, Bunkyo-Ku, Tokyo, Japan.

[1] A. Peterson and D. B. Sinclair, "A single-ended push-pull audio amplifier," PROC. IRE, vol. 40, pp. 7–11; January, 1952.

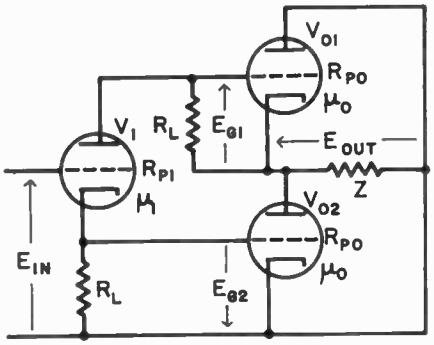

Fig. 3—The equivalent signal-voltage circuit of a single-ended push-pull amplifier with split-load phase inverter driver (type A).

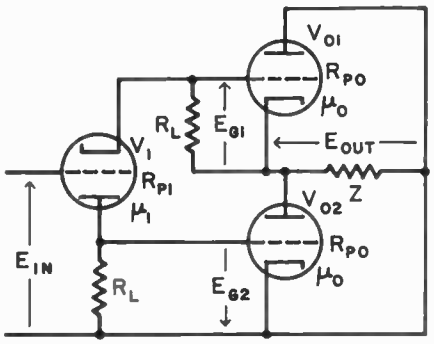

Fig. 4—The equivalent signal-voltage circuit of a single-ended push-pull amplifier with split-load phase inverter driver (type B).

to the midpoint of the series-connected output tubes. As the output voltages E_{out} is proportional to the driving voltage, it may be put that

$$E_{out} = A_0(E_{G1} + E_{G2}),$$

where

$$A_0 = \frac{\mu_0 Z}{R_{P0} + 2Z}.$$

Here, μ_0 is the amplification factor and R_{P0} the plate resistance of the output tubes V_{01} and V_{02}.

Fig. 3 (type A) is the circuit introduced by Peterson and Sinclair,[1,2] and a simple analysis gives

$$E_{G1} = E_{G2} = -\frac{\mu_1 E_{IN} R_L}{(2A_0 + \mu_1 + 2)R_L + R_{P1}}, \quad (1)$$

where μ_1 is the amplification factor, R_{P1} the plate resistance, and R_L the load resistor of V_1.

A similar analysis on the circuit of Fig. 4 (type B) leads to

$$E_{G1} = E_{G2} = \frac{\mu_1 E_{IN} R_L}{\{2(\mu_1 + 1)A_0 + \mu_1 + 2\}R_L + R_{P1}}. \quad (2)$$

In Figs. 3 and 4, the load resistor of V_1 from which the driving voltage for V_{01} is obtained is returned to the cathode of V_{01}. In Figs. 5 and 6, on the other hand, this load resistor is returned to ground, and the load resistor for driving V_{02} is connected to the cathode of V_{01}.

[2] Chai Yeh, "Analysis of a single-ended push-pull audio amplifier," Proc. IRE, vol. 41, pp. 743–747; June, 1953.

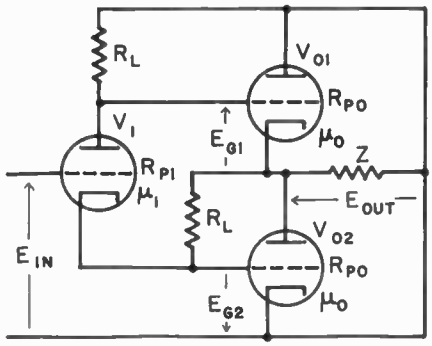

Fig. 5—The equivalent signal-voltage circuit of a single-ended push-pull amplifier with spilt-load phase inverter driver (type C).

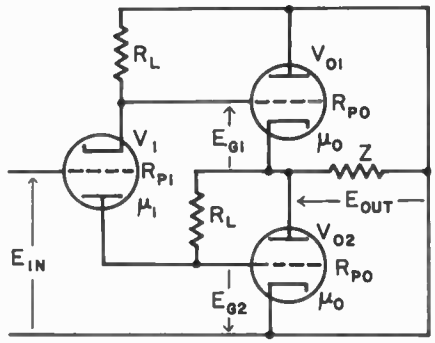

Fig. 6—The equivalent signal-voltage circuit of a single-ended push-pull amplifier with split-load phase inverter driver (type D).

An analysis of the circuit of Fig. 5 (type C) gives[3]

$$E_{G1} = E_{G2} = -\frac{\mu_1 E_{IN} R_L}{(2A_0 + \mu_1 + 2)R_P + (2A_0 + 1)R_{P1}}, \quad (3)$$

and a similar analysis of the circuit of Fig. 6 (type D) gives

$$E_{G1} = E_{G2} = \frac{\mu_1 E_{IN} R_L}{\{2(\mu_1 + 1)A_0 + (\mu_1 + 2)\}R_L + (2A_0 + 1)R_{P1}}. \quad (4)$$

It is interesting to note that (3) and (4) reduce to (1) and (2), respectively, if R_{P1} is substituted for $(2A_0+1)R_{P1}$. The gains of these four drivers are all less than unity.

Cathode-Coupled Phase Inverter Driver[4]

The equivalent signal-voltage circuits of single-ended push-pull amplifiers with the cathode-coupled phase inverter driver are shown in Figs. 7–10. Here again, one of the plate load resistors of the driver stage is returned to the midpoint of the series-connected output stages.

It can be seen from Fig. 7 (type A) that

$$E_{G1} = -\frac{\mu_1 E_{IN}\{R_{L2} + R_{P2} + (\mu_2 + 1)R_K\}R_{L1}}{\Delta_A},$$

[3] Julius Futterman, "An output-transformerless power amplifier," *Jour. AES*, vol. 2, pp. 252–256; October, 1954.

[4] Patent pending (Japan).

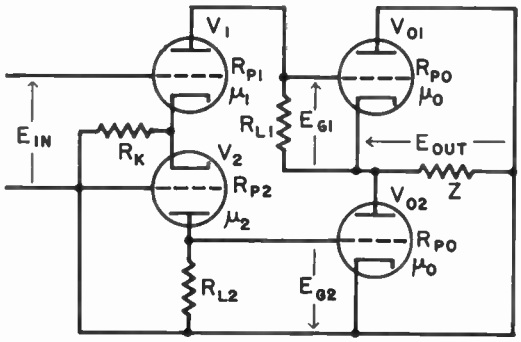

Fig. 7—The equivalent signal-voltage circuit of a single-ended push-pull amplifier with a cathode-coupled phase inverter driver (type A).

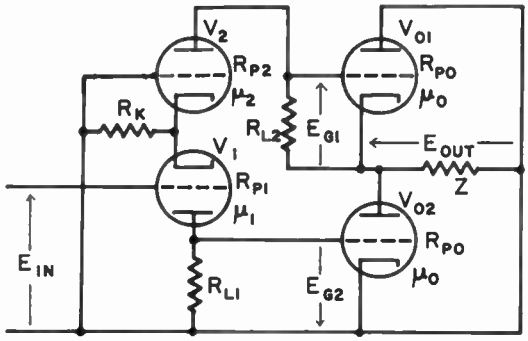

Fig. 8—The equivalent signal-voltage circuit of a single-ended push-pull amplifier with a cathode-coupled phase inverter driver (type B).

and

$$E_{G2} = -\frac{\mu_1 E_{IN}(\mu_2+1)R_K R_{L2}}{\Delta_A},$$

where

$$\Delta_A = \{(A_0+1)R_{L1} + R_{P1} + (\mu_1+1)R_K\} \cdot \{R_{L2} + R_{P2} + (\mu_2+1)R_K\} - \{-A_0 R_{L2} + (\mu_1+1)R_K\}(\mu_2+1)R_K.$$

A_0 is the gain of the output stage, as defined previously. Thus,

$$\frac{E_{G1}}{E_{G2}} = \frac{\{R_{L2} + R_{P2} + (\mu_2+1)R_K\}R_{L1}}{(\mu_2+1)R_K R_{L2}}. \quad (5)$$

Perfect balance is attained by arranging the plate load resistors of the drivers so that the relation

$$\frac{R_{L1}}{R_{L2}} = \frac{(\mu_2+1)R_K}{R_{L2} + R_{P2} + (\mu_2+1)R_K}$$

is satisfied. If the product of $\mu_2 R_K$ is large, a satisfactory balance is obtained using the same value for both R_{L1} and R_{L2}. It should be noted that the balance is not affected by the presence of the output voltage, as seen from the fact that (5) does not include A_0. However, Δ_A is a function of A_0 and the gain of the driver stage is influenced by the variation of the load impedance Z.

For the circuit of Fig. 8 (type B),

$$E_{G1} = \frac{\mu_1 E_{IN}\{-A_0 R_{L1} + (\mu_2+1)R_K\}R_{L2}}{\Delta_B},$$

and

$$E_{G2} = \frac{\mu_1 E_{IN}\{(A_0+1)R_{L2} + R_{P2} + (\mu_2+1)R_K\}R_{L1}}{\Delta_B},$$

where

$$\Delta_B = \{R_{L1} + R_{P1} + (\mu_1+1)R_K\} \cdot \{(A_0+1)R_{L2} + R_{P2} + (\mu_2+1)R_K\} - (\mu_1+1)R_K\{-A_0 R_{L1} + (\mu_2+1)R_K\}.$$

Then,

$$\frac{E_{G1}}{E_{G2}} = \frac{\{-A_0 R_{L1} + (\mu_2+1)R_K\}R_{L2}}{\{(A_0+1)R_{L2} + R_{P2} + (\mu_2+1)R_K\}R_{L1}}. \quad (6)$$

An analysis of the circuit of Fig. 9 (Type C) leads to

$$E_{G1} = -\frac{\mu_1 E_{IN}}{(2A_0+1)\Delta_c} \cdot \left[(A_0+1)\left\{\left(\frac{A_0+1}{2A_0+1}\right)R_{L2} + R_{P2} + (\mu_2+1)R_K\right\}R_{L1} - A_0\left\{\left(\frac{A_0}{2A_0+1}\right)R_{L1} + (\mu_2+1)R_K\right\}R_{L2}\right]$$

and

$$E_{G2} = -\frac{\mu_1 E_{IN}}{(2A_0+1)\Delta^c} \cdot \left[-A_0\left\{\left(\frac{A_0+1}{2A_0+1}\right)R_{L2} + R_{P2} + (\mu_2+1)R_K\right\}R_{L1} + (A_0+1)\left\{\left(\frac{A_0}{2A_0+1}\right)R_{L1} + (\mu_2+1)R_K\right\}R_{L2}\right],$$

where

$$\Delta_c = \{R_{L1} + R_{P1} + (\mu_1+1)R_K\} \cdot \left\{\left(\frac{A_0+1}{2A_0+1}\right)R_{L2} + R_{P2} + (\mu_2+1)R_K\right\} - (\mu_1+1)R_K\left\{\left(\frac{A_0}{2A_0+1}\right)R_{L1} + (\mu_2+1)R_K\right\}.$$

Thus,

$$\frac{E_{G1}}{E_{G2}} = \frac{(A_0+1)\left\{\left(\frac{A_0+1}{2A_0+1}\right)R_{L2} + R_{P2} + (\mu_2+1)R_K\right\}R_{L1} - A_0\left\{\left(\frac{A_0}{2A_0+1}\right)R_{L1} + (\mu_2+1)R_K\right\}R_{L2}}{-A_0\left\{\left(\frac{A_0+1}{2A_0+1}\right)R_{L2} + R_{P2} + (\mu_2+1)R_K\right\}R_{L1} + (A_0+1)\left\{\left(\frac{A_0}{2A_0+1}\right)R_{L1} + (\mu_2+1)R_K\right\}R_{L2}}. \quad (7)$$

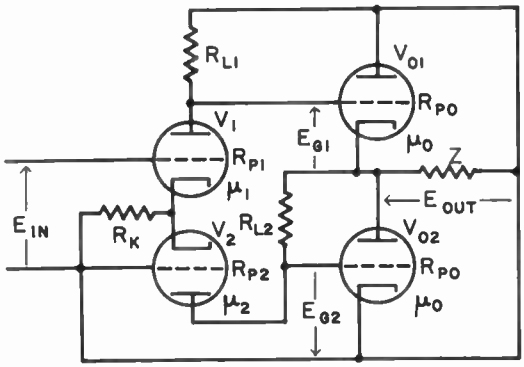

Fig. 9—The equivalent signal-voltage circuit of a single-ended push-pull amplifier with a cathode-coupled phase inverter driver (type C).

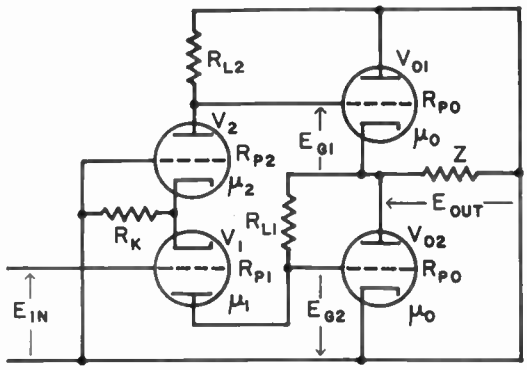

Fig. 10—The equivalent signal-voltage circuit of a single-ended push-pull amplifier with a cathode-coupled phase inverter driver (type D).

Similarly, the circuit of Fig. 10 (type D) is analyzed to give

$$E_{G1} = \frac{\mu_1 E_{IN}}{(2A_0+1)\Delta_D}\left[-A_0\{R_{L2}+R_{P2}+(\mu_2+1)R_K\}R_{L1} + (A_0+1)(\mu_2+1)R_K R_{L2}\right]$$

and

$$E_{G2} = \frac{\mu_1 E_{IN}}{(2A_0+1)\Delta_D}\left[(A_0+1)\{R_{L2}+R_{P2}+(\mu_2+1)R_K\}R_{L1} - A_0(\mu_2+1)R_K R_{L2}\right],$$

where

$$\Delta_D = \left\{\left(\frac{A_0+1}{2A_0+1}\right)R_{L1}+R_{P1}+(\mu_1+1)R_K\right\}\{R_{L2}+R_{P2}+(\mu_2+1)R_K\} - \left\{\left(\frac{A_0}{2A_0+1}\right)R_{L2}+(\mu_1+1)R_K\right\}(\mu_2+1)R_K.$$

Thus,

$$\frac{E_{G1}}{E_{G2}} = \frac{-A_0\{R_{L2}+R_{P2}+(\mu_2+1)R_K\}R_{L1}+(A_0+1)(\mu_2+1)R_K R_{L2}}{(A_0+1)\{R_{L2}+R_{P2}+(\mu_2+1)P_K\}R_{L1}-A_0(\mu_2+1)R_K R_{L2}}. \quad (8)$$

In the circuits of Figs. 8–10, the balance of the driving voltages is affected by E_{out}. However, it is still possible to reduce this effect to a negligible degree by making the product $\mu_2 R_K$ large.

It is not easy to make direct comparison among Eqs. (5)–(8). If the two plate load resistor R_{L1} and R_{L2} of the driver stage are made equal, these four equations reduce to

$$\frac{E_{G1}}{E_{G2}} = \frac{R_L+R_{P2}+(\mu_2+1)R_K}{(\mu_2+1)R_K} > 1, \quad (5')$$

$$\frac{E_{G1}}{E_{G2}} = \frac{-A_0 R_L+(\mu_2+1)R_K}{(A_0+1)R_L+R_{P2}+(\mu_2+1)R_K} < 1, \quad (6')$$

$$\frac{E_{G1}}{E_{G2}} = \frac{R_L+(A_0+1)R_{P2}+(\mu_2+1)R_K}{-A_0 R_{P2}+(\mu_2+1)R_K} > 1, \quad (7')$$

and

$$\frac{E_{G1}}{E_{G2}} = \frac{-A_0 R_L - A_0 R_{P2}+(\mu_2+1)R_K}{(A_0+1)R_K+(A_0+1)R_{P2}+(\mu_2+1)R_K} < 1, \quad (8')$$

respectively, where

$$R_L = R_{L1} = R_{L2}.$$

Now, it is evident that the conditions for a satisfactory balance are given by:

Type	Condition
A	$(\mu_2+1)R_K \gg R_L + R_{P2}$
B	$(\mu_2+1)R_K \gg (2A_0+1)R_L + R_{P2}$
C	$(\mu_2+1)R_K \gg R_L + (2A_0+1)R_{P2}$
D	$(\mu_2+1)R_K \gg (2A_0+1)(R_L+R_{P2})$.

Extended Cathode-Coupled Phase Inverter Driver[5]

Figs. 11 and 12, p. 166, are equivalent signal-voltage circuits of the single-ended push-pull amplifiers with the extended cathode-coupled phase inverter driver. The driver differs from the cathode-coupled phase inverter driver in that the grid of V_2 is not grounded, but rather connected to the plate of V_3, the grid voltage of which is supplied from the common cathode resistor R_K. Because of the phase reversal from the grid to the plate of V_3, the grid voltage of V_3 is in the correct phase for improving the balance of the driving voltages E_{G1} and E_{G2}.

In the circuit of Fig. 11 (type A)

$$E_{G1} = -\frac{\mu_1 E_{IN}[R_{L2}+R_{P2}+\{\mu_2(A+1)+1\}R_K]R_{L1}}{\Delta_{AE}},$$

[5] Hiroshi Amemiya, "Extended cathode-coupled phase inverter and its application to single-ended push-pull amplifiers," scheduled for publication *Jour. AES*, April, 1955.

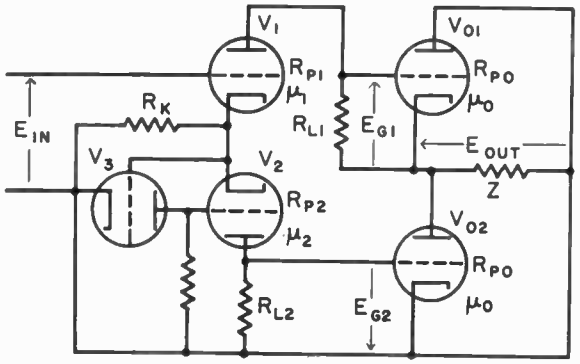

Fig. 11—The equivalent signal-voltage circuit of a single-ended push-pull amplifier with an extended cathode-coupled phase inverter driver (type A).

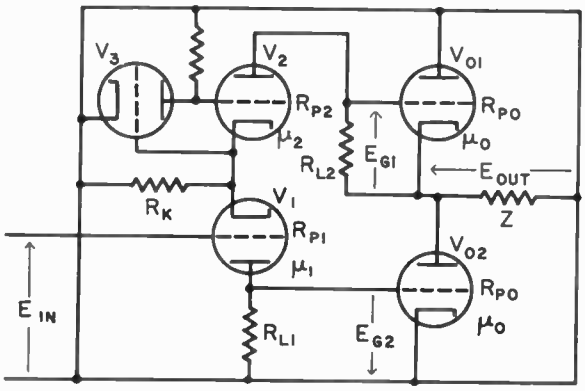

Fig. 12—The equivalent signal-voltage circuit of a single-ended push-pull amplifier with an extended cathode-coupled phase inverter driver (type B).

and

$$E_{G2} = -\frac{\mu_1 E_{IN}\{\mu_2(A+1)+1\}R_K R_{L2}}{\Delta_{AE}},$$

where

$$\Delta_{AE} = [(A_0+1)R_{L1} + R_{P1} + (\mu_1+1)R_K] \cdot [R_{L2} + R_{P2} + \{\mu_2(A+1)+1\}R_K] - \{-A_0 R_{L2} + (\mu_1+1)R_K\}\{\mu_2(A+1)+1\}R_K$$

and A is the gain of V_3.

$$\frac{E_{G1}}{E_{G2}} = \frac{[R_{L2} + R_{P2} + \{\mu_2(A+1)+1\}R_K]R_{L1}}{\{\mu_2(A+1)+1\}R_K R_{L2}}. \quad (9)$$

The balance is not affected by the output voltage E_{out}, as in the case with the type-A cathode-coupled phase inverter driver.

The balance is perfect when

$$\frac{R_{L1}}{R_{L2}} = \frac{\{\mu_2(A+1)+1\}R_K}{R_{L2} + R_{P2} + \{\mu_2(A+1)+1\}R_K}.$$

It is easily seen that even when R_K is small, if the product $\mu_2 A$ is large, a very good balance is obtained using the same value for both R_{L1} and R_{L2}.

Similar analysis of the circuit of Fig. 12 (type B) gives

$$E_{G1} = \frac{\mu_1 E_{IN}[-A_0 R_{L1} + \{\mu_2(A+1)+1\}R_K]R_{L2}}{\Delta_{BE}}$$

and

$$E_{G2} = \frac{\mu_1 E_{IN}[(A_0+1)R_{L2} + R_{P2} + \{\mu_2(A+1)+1\}R_K]R_{L1}}{\Delta_{BE}},$$

where

$$\Delta_{BE} = \{R_{L1} + R_{P1} + (\mu_1+1)R_K\} \cdot [(A_0+1)R_{L2} + R_{P2} + \{\mu_2(A+1)+1\}R_K] - (\mu_1+1)R_K[-A_0 R_{L1} + \{\mu_2(A+1)+1\}R_K].$$

Then

$$\frac{E_{G1}}{E_{G2}} = \frac{[-A_0 R_{L1} + \{\mu_2(A+1)+1\}R_K]R_{L2}}{[(A_0+1)R_{L2} + R_{P2} + \{\mu_2(A+1)+1\}R_K]R_{L1}}. \quad (10)$$

In this case the balance is affected to a certain extent by E_{out}. It is possible, however, to obtain a good balance using the same value for R_{L1} and R_{L2} if $\mu_2 A R_K$ is large.

It is obvious that (9) and (10) reduce to (5) and (6) respectively, if A is put to zero. A careful comparison of the corresponding equations shows that the extended cathode-coupled phase inverter is equivalent to the cathode-coupled phase inverter, provided that the amplification factor of V_2 is multiplied by a factor of $(A+1)$, where A is the gain of V_3.

Although not presented here, type-C and type-D connections are possible, corresponding to the type-C and type-D cathode-coupled phase inverter drivers. The ratios of the driving voltages E_{G1} and E_{G2} with these driver connections may be obtained by substituting $(A+1)\mu_2$ for μ_2 in (7) and (8).

Coulter Driver[6]

As described before, the difficulty in driving single-ended push-pull stage lies in the fact that the output tubes V_{01} and V_{02} are not balanced, so far as the signal-voltage levels of the electrodes measured from the ground are concerned. If driving voltages which are balanced with respect to the ground are applied to the output stage, the upper tube V_{01} works somewhat like a cathode follower and the push-pull condition is not satisfied. In the Coulter driver, a phase inverter is combined with either a degenerative or a regenerative circuit which compensates this unbalance. Figs. 13 and 14, p. 167, are equivalent signal-voltage circuits of the single-ended push-pull amplifiers with the Coulter driver.

In Fig. 13, the input voltage for the upper tube V_{01} is also applied to the grid of V_1 in order to get a phase-reversed driving voltage for the lower tube V_{02}. At the same time, the output voltage is fed back to the cathode of V_1 in a degenerative fashion. Here, K_1 and K_0 are the voltage dividing ratios at the input and the output, respectively. Usually the load Z is not tapped and the feedback voltage is taken from the arm of a potentiometer connected across Z. It is assumed throughout this

[6] W. H. Coulter, "Amplifier circuit having series-connected tubes," U. S. Pat. 2,659,775.

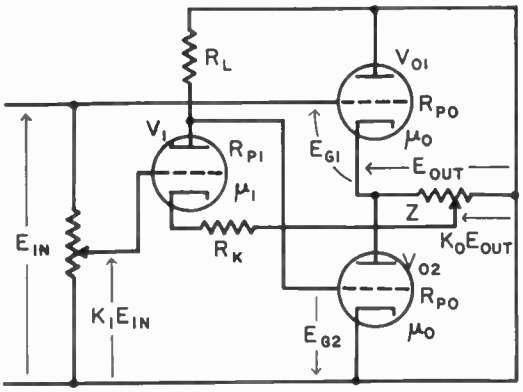

Fig. 13—The equivalent signal-voltage circuit of a single-ended push-pull amplifier with the Coulter driver (degenerative type).

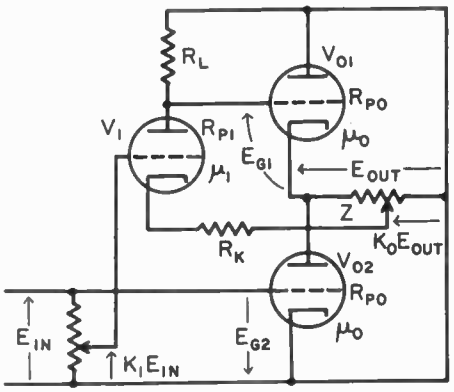

Fig. 14—The equivalent signal-voltage circuit of a single-ended push-pull amplifier with the Coulter driver (regenerative type).

paper that the output impedance of the output stage is very low. Then, Thevenin's theorem shows that the resistance of the potentiometer may be included in the cathode resistor R_K with the feedback voltage directly taken from the tap on the load impedance Z.

Solving the circuit for balanced driving voltage, the following equation is obtained:

$$R_L\{\mu_1K_I(2A_0 + 1) - 2(\mu_1 + 1)K_0A_0\} = R_L + R_{P1} + (\mu_1 + 1)R_K,$$

where

$$A_0 = \frac{\mu_0 Z}{R_{P0} + 2Z}.$$

At first sight it might seem that there are an infinite number of combinations of K_1 and K_0 that give balanced driving voltage. However, it should be recalled here that the balance should not be affected by the variation of the load impedance. Differentiation of the equation with respect to A_0 gives

$$R_L\{2\mu_1K_I - 2(\mu_1 + 1)K_0\} = 0,$$

or

$$K_0 = \frac{\mu_1}{\mu_1 + 1}K_I.$$

Then the satisfactory combination of the dividing ratios is given by

$$\left.\begin{aligned} K_I &= \frac{R_L + R_{P1} + (\mu_1 + 1)R_K}{\mu_1 R_L} \text{ and} \\ K_0 &= \frac{R_L + R_{P1} + (\mu_1 + 1)R_K}{(\mu_1 + 1)R_L}. \end{aligned}\right\} \quad (11)$$

Under this condition

$$E_{G1} = E_{G2} = \frac{R_{P0} + 2Z}{R_{P0} + 2(\mu_0 + 1)Z}E_{IN}.$$

The circuit of Fig. 14 employs positive feedback, and may be analyzed in a similar manner. The balancing condition is given by

$$\{\mu_1K_I + 2(\mu_1 + 1)K_0A_0\}R_L = (2A_0 + 1)\{R_L + R_{P1} + (\mu_1 + 1)R_K\}.$$

Differentiation of the equation with respect to A_0 leads to

$$2(\mu_1 + 1)K_0R_L = 2\{R_L + R_{P1} + (\mu_1 + 1)R_K\}.$$

Thus, the required combination of the dividing ratios is

$$\left.\begin{aligned} K_0 &= \frac{R_L + R_{P1} + (\mu_1 + 1)R_K}{(\mu_1 + 1)R_L} \text{ and} \\ & R_L + R_{P1} + \frac{(\mu_1 + 1)R_K}{\mu_1 R_1} \end{aligned}\right\} \quad (12)$$

Under this condition,

$$E_{G1} = E_{G2} = -E_{IN}.$$

As might be expected from inspection of the circuit connections, (11) and (12) are identical. In the circuit of Fig. 14, misadjustment of positive feedback might cause instability. When K_0 is made such that

$$K_0 = \frac{R_L + R_{P1} + (\mu_1 + 1)R_K}{(\mu_1 + 1)R_L} \cdot \frac{R_{P0} + (\mu_0 + 2)Z}{\mu_0 Z},$$

the amplifier becomes unstable.

Conclusion

Drivers for a single-ended push-pull stage have been analyzed with stress on the balance of the driving voltages. Actually, other factors, such as gain, distortion, and frequency characteristics must be considered in the selection of a suitable driver for a particular case.

The author has no intention of insisting that the drivers presented in the paper are the only possible drivers for the single-ended push-pull connection. Rather, he is eagerly looking forward to the advent of new and better drivers for this push-pull circuit.

Contributors

Hiroshi Amemiya (S'52–A'53) was born in Tokyo, Japan, in 1927. He attended the University of Tokyo to study electrical engineering and received the degree of Bachelor of Engineering (Kogaku-shi) in 1948. From 1948 to 1949 Mr. Amemiya was employed by the Japan Victor Co., where he was concerned with the production of loudspeakers. In 1950 he returned to the University of Tokyo for further study in electrical communications engineering. He came to the United States in 1952 to participate in the International Educational Exchange Program of the U.S. Government. While in the United States he studied at Cornell University, and received the degree of Master of Science in 1954. At present he is a graduate student of the University of Tokyo.

HIROSHI AMEMIYA

Mr. Amemiya is a member of the Institute of Electrical Communication Engineers of Japan, the AES, and Sigma Xi.

❖

Robert L. Trent (M'45) was born March 21, 1919, in New York City. He joined Bell Telephone Laboratories in 1941, having received the B.S. degree in electrical engineering from the School of Engineering, Columbia University. In 1946 he received the M.S. degree from the same institution.

R. L. TRENT

From the time he joined the Laboratories until 1947 Mr. Trent was concerned almost exclusively with war developments, taking part in the development of sonar, airborne radar, and pulse-code-modulation communication equipment. From 1947 to 1949 he worked on various aspects of short- and long-haul radio-relay television links. In 1950 he entered electronic device development work.

Mr. Trent is presently engaged in exploratory development work in transistor circuitry. Previously he was concerned with development of transistor devices.

Mr. Trent received honorable mention in the Eta Kappa Nu awards to Outstanding Young Electrical Engineers for 1951. He is a member of the American Institute of Electrical Engineers, and Eta Kappa Nu.

❖

For a photograph and biography of **Benjamin B. Bauer,** see the Award Recipients Section of the July-August, 1955, issue of the TRANSACTIONS ON AUDIO.

INSTITUTIONAL LISTINGS

The IRE Professional Group on Audio is grateful for the assistance given by the firms listed below, and invites application for Institutional Listing from other firms interested in Audio Technology.

ELECTRO-VOICE, INC., Buchanan, Michigan
Microphones, Pickups, Speakers, Television Boosters, Acoustic Devices

GENERAL CERAMICS CORPORATION, Keasbey, New Jersey
Technical Ceramics—Steatites and Aluminum, Ferramics, Solderseals

JENSEN MANUFACTURING COMPANY, 6601 South Laramie Avenue, Chicago 38, Illinois
Loudspeakers, Reproducer Systems, Enclosures

KLIPSCH AND ASSOCIATES, Box 64, Hope, Arkansas
Wide Range Corner Horn Loudspeaker Systems, Corner Horns

JAMES B. LANSING SOUND, INC., 2439 Fletcher Drive, Los Angeles 39, California
Loudspeakers and Transducers of All Types

MAGNECORD, INC., 360 North Michigan Avenue, Chicago 1, Illinois
Special & Professional Magnetic Tape Recording Equipment

PERMOFLUX CORPORATION, 4900 West Grand Avenue, Chicago 39, Illinois
Loudspeakers, Headphones, Cee-Cors (Hipersil Transformer Cores)

SHURE BROTHERS, INC., 225 West Huron Street, Chicago 10, Illinois
Microphones, Pickups, Recording Heads, Acoustic Devices

THE TURNER COMPANY, Cedar Rapids, Iowa
Microphones, Television Boosters, Acoustic Devices

UNITED TRANSFORMER COMPANY, 150 Varick Street, New York, New York
Transformers, Filters and Reactors

UNIVERSITY LOUDSPEAKERS, INC., 80 South Kenisco Avenue, White Plains, New York
Manufacturers of Public Address and High Fidelity Loudspeakers

INSTITUTIONAL LISTINGS

ALLIED RADIO, 833 West Jackson Blvd., Chicago 7, Illinois
Everything in Radio, Television, and Industrial Electronics

ALTEC LANSING CORPORATION, 9356 Santa Monica Blvd., Beverly Hills, California
Microphones, Speakers, Amplifiers, Transformers, Speech Input

AMPEX CORPORATION, 934 Charter Street, Redwood City, California
Magnetic Tape Recorders for Audio and Test Data

AMPLIFIER CORPORATION OF AMERICA, 398 Broadway, New York 13, New York
Manufacturers of Magnetic Tape Recorders and Manufacturing Engineers

AUDIOPHILE RECORDS, Saukville, Wisconsin
High Quality Disc Recordings for Wide Range Equipment

BALLANTINE LABORATORIES, INC., Fanny Road, Boonton, New Jersey
Electronic Voltmeters, Decade Amplifiers, Voltage Calibrators, Multipliers, Shunts

CINEMA ENGINEERING CO., Division Aerovox Corp., 1100 Chestnut St., Burbank, California
Equalizers, Attenuators, Communication Equipment

THE DAVEN COMPANY, 191 Central Avenue, Newark 4, New Jersey
Attenuators, Potentiometers, Resistors, Rotary Switches, Test Equipment

Charge for listing in six consecutive issues of the TRANSACTIONS—$25.00. Application for listing may be made to the Chairman of the IRE-PGA Ways and Means Committee, Michel Copel, 156 Olive St., Huntington, L.I., N.Y.

(Please see inside back cover for additional listings.)